

A CAHN–HILLIARD–WILLMORE PHASE FIELD MODEL FOR NON-ORIENTED INTERFACES

ELIE BRETIN, ANTONIN CHAMBOLLE, AND SIMON MASNOU

ABSTRACT. We investigate a new phase field model for representing non-oriented interfaces, approximating their area and simulating their area-minimizing flow. Our contribution is related to the approach proposed in [22] that involves ad hoc neural networks. We show here that, instead of neural networks, similar results can be obtained using a more standard variational approach that combines a Cahn-Hilliard-type functional involving an appropriate non-smooth potential and a Willmore-type stabilization energy.

We show some properties of this phase field model in dimension 1 and, for radially symmetric functions, in arbitrary dimension. We propose a simple numerical scheme to approximate its L^2 -gradient flow. We illustrate numerically that the new flow approximates fairly well the mean curvature flow of codimension 1 or 2 interfaces in dimensions 2 and 3.

1. INTRODUCTION

A phase field approach was proposed in [22] to represent non-oriented interfaces and simulate their area-minimizing flow. The approach is based on ad hoc neural networks that are trained to approximate an evolution by mean curvature flow on a fixed time step. The main contribution of the current paper is to propose an alternative to neural networks based on a new but more standard variational phase field model. This model combines a Cahn-Hilliard-type energy to approximate the area and a Willmore-type energy to stabilize the phase field profile. The Cahn-Hilliard-type energy involves a nonstandard potential with one well at 0 and an obstacle at $\frac{1}{4}$. The gradient flow associated with the proposed model is numerically similar to the mean curvature flow. We establish some analytical results which support, in part, the numerical observations.

Given $d \in \mathbb{N}^*$, $\varepsilon > 0$ and $Q \subset \mathbb{R}^d$ an open and bounded set, we consider the phase field functional \mathcal{E}_ε defined for every $u \in W^{2,2}(Q)$ such that $u \leq \frac{1}{4}$ a.e. by

$$\mathcal{E}_\varepsilon(u, Q) = \int_Q \left(\frac{\varepsilon}{2} |\nabla u|^2 + \frac{1}{\varepsilon} F(u) \right) dx + \frac{\sigma_\varepsilon}{2\varepsilon} \int_Q \left(\varepsilon \Delta u - \frac{1}{\varepsilon} F'(u) \right)^2 dx,$$

where σ_ε is any positive function of ε such that $\varepsilon^2/\sigma_\varepsilon \rightarrow 0$ as $\varepsilon \rightarrow 0^+$, and the potential F is nonsmooth and defined as

$$F(s) = \begin{cases} s^2(\frac{1}{2} - 2s) & \text{if } s \leq \frac{1}{4} \\ +\infty & \text{otherwise} \end{cases}$$

The main theoretical contribution of this work is a convergence analysis of \mathcal{E}_ε as $\varepsilon \rightarrow 0^+$ in dimension $d = 1$, and in the radially symmetric case in higher dimension $d \geq 2$. We also

Date: December 23, 2024.

2020 Mathematics Subject Classification. 74N20, 35A35, 53E10, 53E40, 65M32, 35A15.

Key words and phrases. Phase field approximation, mean curvature flow of non-oriented interfaces, Cahn-Hilliard energy, Willmore energy, non smooth potential, numerical approximation.

introduce a numerical scheme to approximate the L^2 -gradient flow of \mathcal{E}_ε

$$\begin{cases} u_t &= -\mu + \sigma_\varepsilon(\Delta\mu - \frac{1}{\varepsilon^2}F''(u)\mu), \\ \mu &= -\Delta u + \frac{1}{\varepsilon^2}F'(u), \end{cases}$$

and we illustrate with several numerical simulations that this new model provides a fairly good approximation of the mean curvature flow of non-oriented interfaces of codimension 1 or 2 in dimensions $d = 2$ or $d = 3$.

In the case where the potential F is replaced with a smooth and classical double-well potential such as $W(s) = \frac{1}{2}s^2(1-s)^2$, it is well known that the Γ -limit of \mathcal{E}_ε in dimensions $N = 2, 3$ coincide on sets with smooth boundary with a weighted sum of their perimeter and Willmore energy [7, 51, 24].

In contrast with W , our potential F has a well at $s = 0$ with $F'(0) = 0$ and an obstacle at $s = \frac{1}{4}$ with $F'(\frac{1}{4}) < 0$ (considering the left-derivative of F at $\frac{1}{4}$). If we consider only the first term of the functional, i.e.

$$\int_Q \left(\frac{\varepsilon}{2} |\nabla u|^2 + \frac{1}{\varepsilon} F(u) \right) dx,$$

the classical argument of Modica and Mortola [47] can be easily adapted to prove the Γ -convergence to the perimeter functional (up to a constant multiplier). However, adding the Willmore term changes everything, as it penalises the $\frac{1}{4}$ -phase so that any minimizing sequence must converge to 0 almost everywhere. In the limit, the $\frac{1}{4}$ -phase has zero volume.

Other phase field models, such as in [3, 15], yield one phase only in the limit (up to a negligible set). For instance, the approximation of the Mumford-Shah functional by Ambrosio-Tortorelli's model [3] involves the single-well potential $G(s) = \frac{1}{2}(s-1)^2$ and an auxiliary phase field. In the limit, the 1-phase connects with the (negligible) 0-phase through a non-smooth profile with infinite derivative at 0. It is a major difference with our potential F which guarantees smooth connecting profiles between phases 0 and $\frac{1}{4}$. This smoothness grants the possibility to use the Willmore energy, whose purpose is then to stabilise the optimal phase field profile, as will be shown from our (partial) theory and the numerical experiments.

As we are going to illustrate numerically, the main interest of the functional \mathcal{E}_ε together with the proposed scaling of ε and σ_ε is that the associated L^2 -gradient flow provides a good numerical approximation of the mean curvature flow of non oriented interfaces, possibly with triple points. An advantage of the phase field approach is its versatility: the flow could be easily coupled with inclusion constraints as in [22] to approximate solutions such as those of the Steiner or Plateau problems.

1.1. Classical phase field models for the perimeter and the Willmore energy. It follows from the results of Modica and Mortola [47, 46] that, for a class of smooth double-well potentials W that includes $W(s) = \frac{1}{2}s^2(1-s)^2$, the Γ -limit in $L^1(Q)$ of the so-called Cahn-Hilliard functional

$$P_\varepsilon(u) = \begin{cases} \int_Q \left(\frac{\varepsilon}{2} |\nabla u|^2 + \frac{W(u)}{\varepsilon} \right) dx & \text{if } u \in W^{1,2}(Q) \\ +\infty & \text{otherwise in } L^1(Q) \end{cases}$$

is $c_0 P(u)$ where

$$P(u) = \begin{cases} |Du|(Q) & \text{if } u \in \text{BV}(Q, \{0, 1\}) \\ +\infty & \text{otherwise in } L^1(\Omega) \end{cases}$$

and $c_0 = \int_0^1 \sqrt{2W(s)} ds$. In particular, if $\Omega \subset \mathbb{R}^d$ has finite perimeter in the bounded set Q , thus $u := \mathbb{1}_\Omega \in \text{BV}(Q, \{0, 1\})$, one can build a sequence of functions $(u_\varepsilon) \in W^{1,2}(Q)$ such that $u_\varepsilon \rightarrow u \in L^1(Q)$ and $P_\varepsilon(u_\varepsilon) \rightarrow c_0 |Du|(\Omega) = c_0 P(\Omega, Q)$ as $\varepsilon \rightarrow 0$, with $P(\Omega, Q)$ the perimeter of Ω in Q .

A time-dependent smooth domain $\Omega(t) \subset \mathbb{R}^d$ evolves under the classical mean curvature flow if its inner normal velocity at every point $x \in \partial\Omega(t)$ is the scalar mean curvature $H_{\Omega(t)}(x)$ of $\partial\Omega(t)$ at x (with the orientation convention that the scalar mean curvature on the boundary of a convex domain is positive). This evolution may be understood as the L^2 -gradient flow of the perimeter $P(\Omega(t))$. Now, P can be approximated by the Cahn-Hilliard energy P_ε , and the L^2 -gradient flow of P_ε leads to the celebrated Allen-Cahn equation [2] which reads as, up to a time rescaling:

$$\partial_t u_\varepsilon = \Delta u_\varepsilon - \frac{1}{\varepsilon^2} W'(u_\varepsilon).$$

A formal asymptotic expansion of the solution u_ε to the Allen-Cahn equation near the interface $\partial\Omega_\varepsilon(t) := \partial \{u_\varepsilon(\cdot, t) \geq \frac{1}{2}\}$ gives (see [4])

$$u_\varepsilon(x, t) = q\left(\frac{\text{dist}(x, \Omega_\varepsilon(t))}{\varepsilon}\right) + O(\varepsilon^2),$$

where $\text{dist}(\cdot, \Omega_\varepsilon(t))$ is the signed distance function to $\Omega_\varepsilon(t)$ (negative inside, positive outside) and $q : \mathbb{R} \rightarrow [0, 1]$ is the so-called *optimal profile* which minimizes the parameter-free one-dimensional Allen-Cahn energy under some constraints:

$$q = \arg \min_p \left\{ \int_{\mathbb{R}} \left(\frac{1}{2} |p'(s)|^2 + W(p(s)) \right) ds, p \in C^{0,1}(\mathbb{R}), p(-\infty) = 1, p(0) = \frac{1}{2}, p(+\infty) = 0 \right\}.$$

Furthermore, the velocity V_ε of the boundary $\partial\Omega_\varepsilon(t)$ satisfies

$$V_\varepsilon(t) = H_\varepsilon(t) + O(\varepsilon^2),$$

where $H_\varepsilon(t)$ denotes the scalar mean curvature on $\partial\Omega_\varepsilon(t)$, which suggests that the Allen-Cahn equation approximates the mean curvature flow with an error of order ε^2 [4].

Rigorous proofs of convergence of the Allen-Cahn flow to the smooth mean curvature flow for short times (in particular before the onset of singularities) have been presented in [27, 33, 8]. More precisely, given an initial smooth set Ω_0 , its mean curvature flow $\Omega(t)$, an initial condition $u_0 = q\left(\frac{\text{dist}(x, \Omega_0)}{\varepsilon}\right)$, the solution $u_\varepsilon(\cdot, t)$ to the Allen-Cahn equation with $u_\varepsilon(\cdot, 0) = u_0$, and the evolving set $\Omega_\varepsilon(t) = \{u_\varepsilon(\cdot, t) \geq \frac{1}{2}\}$, a quasi-optimal error on the Hausdorff distance between $\Omega(t)$ and $\Omega_\varepsilon(t)$ is proved in these papers, namely

$$\text{dist}_{\mathcal{H}}(\Omega(t), \Omega_\varepsilon(t)) \leq C\varepsilon^2 |\log(\varepsilon)|^2,$$

where the constant C depends on the regularity of Ω_0 .

The use of less regular potentials has been proposed, see for instance [10], to guarantee solutions with better physical or mathematical properties. For example, the convergence analysis of the Allen-Cahn equation using a double obstacle potential

$$W(s) = \begin{cases} s(1-s) & \text{if } s \in [0, 1], \\ +\infty & \text{otherwise} \end{cases}$$

is carried out in [29, 35], where it is proved that solutions, which are constrained to remain valued in $[0, 1]$, have finite transition zone around the interface $\partial\Omega_\varepsilon$ such that $\text{dist}_{\mathcal{H}}(\Omega(t), \Omega_\varepsilon(t)) \leq C\varepsilon^2$.

The use of logarithmic potentials in Cahn-Hilliard models for the approximation of surface diffusion flows has been extensively studied in [29], allowing also to guarantee the inclusion property of the phase field solution u_ε and no singularities.

The Willmore energy of a set $\Omega \subset \mathbb{R}^d$ with smooth boundary in Q is defined as

$$\mathcal{W}(\Omega, Q) = \frac{1}{2} \int_{\partial\Omega \cap Q} |H_\Omega(x)|^2 d\mathcal{H}^{d-1},$$

where \mathcal{H}^{d-1} denotes the $(d-1)$ -dimensional Hausdorff measure. Based on a conjecture of De Giorgi [32], several authors [7, 57, 6, 48, 51, 50, 24, 5] have investigated the phase field approximation of \mathcal{W} using a double-well potential such as the function W defined in the introduction. A classical approximation functional is

$$\mathcal{W}_\varepsilon(u) = \begin{cases} \frac{1}{2\varepsilon} \int_Q \left(\varepsilon \Delta u - \frac{W'(u)}{\varepsilon} \right)^2 dx & \text{if } u \in L^1(Q) \cap W^{2,2}(Q) \\ +\infty & \text{otherwise in } L^1(Q). \end{cases}$$

Bellettini and Paolini [7] have proved for this functional a Γ -lim sup property: given a set Ω with smooth boundary, there exists a suitable family of smooth approximations u_ε of $\mathbb{1}_\Omega$ such that the limit of $\mathcal{W}_\varepsilon(u_\varepsilon)$ is, up to a multiplicative constant, the Willmore energy $\mathcal{W}(\Omega, Q)$.

The Γ -lim inf property is much harder to prove, see the various contributions in [57, 6, 48, 51, 50]. In particular, it was proven by Röger and Schätzle in [51] in space dimensions $N = 2, 3$ and, independently, by Nagase and Tonegawa [50] in dimension $N = 2$, that the result holds true for smooth sets. More precisely, given $u = \mathbb{1}_\Omega$ with $\partial\Omega \in C^2(Q)$, and u_ε converging to u in L^1 with a uniform control of $P_\varepsilon(u_\varepsilon)$, then

$$c_0 \mathcal{W}(\Omega, Q) \leq \liminf_{\varepsilon \rightarrow 0^+} \mathcal{W}_\varepsilon(u_\varepsilon).$$

The proof is based on a careful control of the discrepancy measure

$$\xi_\varepsilon = \left(\frac{\varepsilon}{2} |\nabla u|^2 - \frac{W(u)}{\varepsilon} \right) \mathcal{L}^2,$$

which guarantees that the minimizing sequence has the correct phase field profile

$$u_\varepsilon \simeq q(\text{dist}(x, \Omega)/\varepsilon).$$

Then, in Röger & Schätzle's proof, the result follows from a representation with varifolds of the limit measure, a lower semicontinuity argument and the locality property of the generalized mean curvature of integral varifolds. Due to dimensional requirements for Sobolev embeddings and for the control of singular terms, the proof works in dimensions $N = 2, 3$ only. The result in higher dimension is still open.

It was shown, first formally in [45, 59, 24] with asymptotic expansion arguments, then rigorously in [38], that the L^2 -gradient flow of \mathcal{W}_ε ,

$$\begin{cases} \partial_t u_\varepsilon = \Delta \mu_\varepsilon - \frac{1}{\varepsilon^2} W''(u_\varepsilon) \mu_\varepsilon, \\ \mu_\varepsilon = -\Delta u_\varepsilon + \frac{1}{\varepsilon^2} W'(u_\varepsilon), \end{cases}$$

converges to the Willmore flow, i.e. the L^2 -gradient flow of \mathcal{W} , which is characterized by the inner normal velocity

$$V_n = \Delta_{\partial E} H + \|A\|^2 H - \frac{H^3}{2},$$

where H is the mean curvature on ∂E , A is the second fundamental form and $\|A\|^2$ coincides with the sum of the squared principle curvatures.

We are not aware of any use of potentials less regular than $W(s) = s^2(1-s)^2$ for the approximation of the Willmore energy and its associated flow, the lack of regularity being an obstacle to any proof of convergence. The idea of the present article is therefore to go a little deeper into this case. We will show the interest of considering a potential with one well and one obstacle to both bound and stabilize the phase associated to the obstacle.

1.2. Ambrosio-Tortorelli's functional and the case of non oriented interfaces. Some applications, typically free-discontinuity problems, require the minimization of the area of interfaces that are not domain's boundaries and sometimes even not orientable. In such a case, obviously, the Cahn-Hilliard energy cannot be used to approximate the area.

A first typical example is in image segmentation with the Mumford-Shah model [49, 31]. Given a gray-scale image I_0 defined on a domain $Q \subset \mathbb{R}^2$, one seeks for a piecewise smooth approximation v of I_0 by minimizing the Mumford-Shah functional

$$\mathcal{E}^{MS}(v, \Gamma) = \int_Q (v - I_0)^2 dx + \mu \int_{Q \setminus \Gamma} |\nabla v|^2 dx + \eta \mathcal{H}^1(\Gamma).$$

among all pairs (v, Γ) such that

$$\Gamma \subset Q \text{ is closed and } v \in C^1(Q \setminus \Gamma).$$

Ambrosio and Tortorelli proposed in [3] a phase-field approximation of \mathcal{E}^{MS} of the form

$$\mathcal{E}_\varepsilon^{AT}(v, u) = \int_Q (v - I_0)^2 dx + \mu \int_Q u^2 |\nabla v|^2 dx + \eta \mathcal{F}_\varepsilon(u)$$

where the so-called Ambrosio-Tortorelli term \mathcal{F}_ε is defined as

$$\mathcal{F}_\varepsilon(u) = \int_Q \left(\varepsilon |\nabla u|^2 + \frac{1}{4\varepsilon} (1 - u)^2 \right) dx.$$

Ambrosio and Tortorelli proved a Γ -convergence result of $\mathcal{E}_\varepsilon^{AT}$ to \mathcal{E}^{MS} in a suitable functional framework. Intuitively, a phase field minimizer u_ε of $\mathcal{E}_\varepsilon^{AT}$ is of the form $u_\varepsilon = \varphi(\text{dist}(x, \Gamma)/\varepsilon)$ (where dist now denotes the classical distance function), it vanishes on Γ and $\mathcal{F}_\varepsilon(u_\varepsilon)$ approximates the length of Γ . However, unlike the Cahn-Hilliard energy, the term \mathcal{F}_ε considered separately Γ -converges to 0 rather than to the length of Γ . In other words, \mathcal{F}_ε needs to be coupled with additional terms and constraints to approximate the length of Γ , which raises a number of numerical difficulties.

A second example is related to the Steiner problem. Recall that, given a collection of points $a_1, \dots, a_L \in Q$, the associated Steiner problem consists in finding a compact connected set $\Gamma \subset Q$ containing every a_i and having minimal length. It is equivalent to finding the optimal solution to the problem

$$\min_{\Gamma} \{ \mathcal{H}^1(\Gamma), \Gamma \subset Q, \Gamma \text{ connected}, a_i \in \Gamma, \forall i = 1, \dots, L \},$$

Ad hoc variational phase field models for the Steiner problem have recently been introduced, see for instance [14, 13, 11, 12, 25]. The model introduced in [14] involves the Ambrosio-Tortorelli term \mathcal{F}_ε coupled to an additional geodesic term \mathcal{G}_ε that forces the connectedness of Γ :

$$\mathcal{G}_\varepsilon(u) = \frac{1}{\varepsilon} \sum_{i=1}^N \mathbf{D}(u^2; a_0, a_i), \quad \text{with } \mathbf{D}(w; a, b) := \inf_{\Gamma: a \rightsquigarrow b} \int_{\Gamma} w \, d\mathcal{H}^1 \in [0, +\infty].$$

Here the notation $\Gamma : a \rightsquigarrow b$ refers to a rectifiable curve $\Gamma \subset \Omega$ connecting a and b .

Intuitively, and as previously, a phase field minimizer u_ε of $\mathcal{F}_\varepsilon + \mathcal{G}_\varepsilon$ is expected to be of the form $u_\varepsilon = \varphi(\text{dist}(x, \Gamma)/\varepsilon)$ where the geodesic term $\mathcal{G}_\varepsilon(u_\varepsilon)$ forces u_ε to vanish on a set Γ connecting all a_i 's and whose length is approximated by the Ambrosio-Tortorelli term $\mathcal{F}_\varepsilon(u_\varepsilon)$.

The Γ -convergence result proved in [14] suggests that the minimization of this phase field model provides an approximation of a Steiner solution, i.e. a Steiner tree. However, despite the numerical experiments provided in [14, 13] show the ability of the model to approximate solutions of the Steiner problem in dimensions 2, 3, they also show how difficult it is to minimize effectively the geodesic term $\mathcal{G}_\varepsilon(u_\varepsilon)$ to guarantee the connectedness of Γ . The conclusions are quite similar for the approaches developed in [11, 12, 25] based on the measure-theoretic notion of current. In these latter approaches, the connectedness of Γ is ensured by adding a divergence constraint of the form $\text{div}(\tau) = \sum \alpha_i \delta_{a_i}$ for a suitable field τ .

In short, all these models provide reasonable approximations of solutions to the Steiner problem, but the algorithmic cost is rather high and the approximations lack of regularity.

A motivation of this paper is therefore to propose a more straightforward approach that does not need to be coupled with sophisticated constraints, and which is directly related to the approximation of the mean curvature flow of non oriented interfaces.

1.3. Unoriented phase field profile and neural networks. As mentioned above, the key point that limits the effectiveness of phase field methods for approximating minimization problems involving the perimeter of a non oriented set Γ is that they are based on Ambrosio-Tortorelli-type energies which need to be coupled with other terms or constraints to ensure the stability of the optimal phase field profiles. In fact, unlike the Allen-Cahn equation, i.e. the gradient flow of the Cahn-Hilliard energy, which provides good approximations of the mean curvature flow of set boundaries, the gradient flow of the Ambrosio-Tortorelli model is not suitable for approximating the evolution by mean curvature of more general interfaces, in particular interfaces that are not boundaries.

Recently, it was proposed in [22] to design and train suitable neural networks for approximating these latter evolutions. More specifically, using the same notations as above and denoting as $\Gamma(t)$ the mean curvature flow of a smooth, general interface (not necessarily the

boundary of a domain), the general idea in [22] is to train a neural network \mathcal{S}_θ such that

$$\mathcal{S}_\theta \left[-q' \left(\frac{d(x, \Gamma(t))}{\varepsilon} \right) \right] \simeq -q' \left(\frac{d(x, \Gamma(t + \delta_t))}{\varepsilon} \right),$$

where d is now the (unoriented) distance function. The main advantage of using the profile q' is that it does not require any orientation of $\Gamma(t)$. Figure 1.3 illustrates the difference between oriented and non-oriented representations.

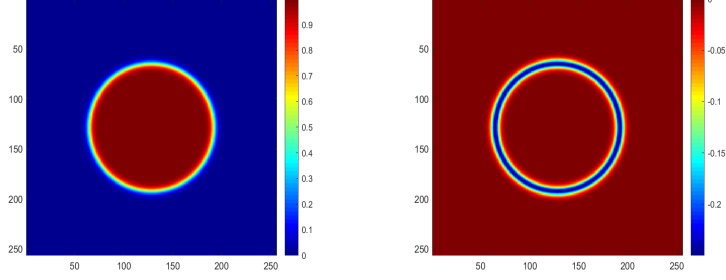


FIGURE 1. Oriented (q , left) and non-oriented ($-q'$, right) phase field approximations of a disk / circle in dimension 2.

The training of \mathcal{S}_θ , i.e. the calibration of its inner parameters, was performed in [22] with a training database made of circles (in dimension 2) or spheres (in dimension 3) whose flow by mean curvature is known exactly.

As for the network structures proposed for \mathcal{S}_θ in [22], they are very simple and inspired by discretisation schemes that alternate diffusion and reaction operations to approximate numerically the solutions to the Allen-Cahn equation. Two typical structures studied in [22] are shown in figure 1.3, where each \mathcal{D} denotes a convolution operation (two different \mathcal{D} in the same network might have different parameters) and \mathcal{R} is a pointwise reaction trainable function (in practice, a 3-layer perceptron).

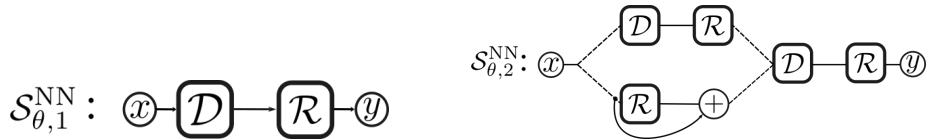


FIGURE 2. Two network structures obtained from first order (left) and second order (right) discretisation schemes of the Allen-Cahn equation

The evaluation of the numerical performances of these networks leads to the following conclusion: oriented mean curvature flows can be learned with either first-order or second-order networks, but only second-order networks are able to learn non oriented mean curvature flows. More precisely, the first-order networks proposed in [22] extend time-discrete approximations of the Allen-Cahn equation

$$u_t = \Delta u - \frac{1}{\varepsilon^2} W'(u),$$

hence the results of [22] suggest that any phase field model of the form

$$u_t = D_1[u] + R_1[u]$$

fails to approximate a non-oriented mean curvature flow. Instead, the good performances of second-order networks (as illustrated in figure 1.3) suggest that a phase field model such as

$$(1.1) \quad \begin{cases} u_t &= D_2[v] + R_3(u)R_2[v], \\ v &= D_1[u] + R_1[u], \end{cases}$$

might be able to approximate non-oriented mean curvature flows.

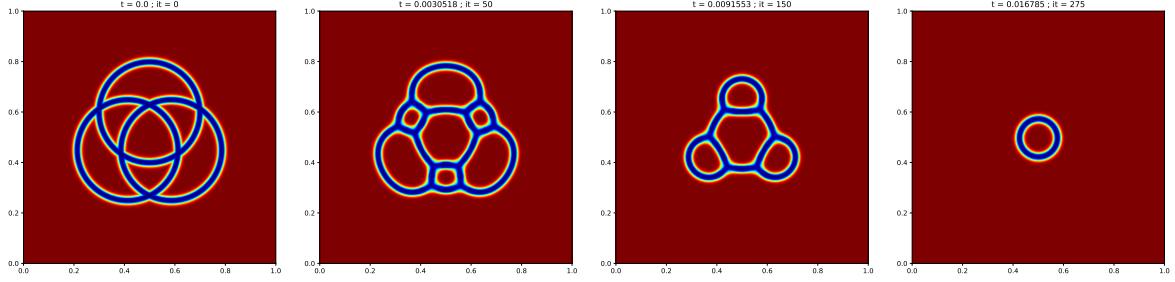


FIGURE 3. Approximation with a second order neural network of the motion by mean curvature of non oriented interfaces.

1.4. Derivation of a new phase field model. Following these observations, let us try to identify a phase field model that would be suitable for the approximation of a nonoriented mean curvature flow. We start with the derivation of an ODE satisfied by the profile $-q'$. Recall that q satisfies

$$q'(s) = -\sqrt{2W(q(s))}, \quad q''(s) = W'(q(s)) \quad \text{and} \quad q(0) = \frac{1}{2},$$

where W is the quadratic smooth potential $W(s) = \frac{1}{2}s^2(1-s)^2$. Exploiting the symmetry of the double-well potential W , it is not difficult to see that

$$q^{(3)}(s) = W''(q(s))q' = (6q(s)^2 - 6q(s) + 1)q'(s) = (1 + 6q'(s))q'(s).$$

This shows that the profile $y = -q'$ is a solution to the equation

$$y''(s) = F'(y(s)),$$

where the potential F is defined as previously by

$$F(s) = \begin{cases} s^2(\frac{1}{2} - 2s) & \text{if } s \leq \frac{1}{4} \\ +\infty & \text{otherwise.} \end{cases}$$

A PDE naturally associated with the above ODE is the Allen-Cahn-type equation

$$u_t = \Delta u - \frac{1}{\varepsilon} F'(u),$$

i.e. the L^2 -gradient flow of the modified Cahn-Hilliard energy obtained by replacing with F the smooth potential W . However, as shown by the numerical experiments performed with neural networks, such a model fails to preserve the profile q' along the iterations.

A simple way to get stability consists in adding to the modified Cahn-Hilliard energy a second-order term that forces the equation $y'' = F'(y')$. More precisely, we consider the following phase field approximation of the perimeter plus Willmore energy:

$$\mathcal{E}_\varepsilon(u, Q) = \int_Q \left(\frac{\varepsilon}{2} |\nabla u|^2 + \frac{1}{\varepsilon} F(u) \right) dx + \frac{\sigma_\varepsilon}{2\varepsilon} \int_Q \left(\varepsilon \Delta u - \frac{1}{\varepsilon} F'(u) \right)^2 dx$$

where the parameter σ_ε must be large enough to guarantee the profile's stability, but not so large that the Willmore term remains negligible compared to the perimeter term. The L^2 -gradient flow of \mathcal{E}_ε writes

$$\begin{cases} u_t &= -\mu + \sigma_\varepsilon \left(\Delta \mu - \frac{1}{\varepsilon^2} F''(u) \mu \right), \\ \mu &= -\Delta u + \frac{1}{\varepsilon^2} F'(u), \end{cases}$$

which is exactly of the proposed form (1.1).

1.5. Outline of the paper. The convergence analysis of \mathcal{E}_ε as $\varepsilon \rightarrow 0$ is carried out in the next section. We first show that the limit energy concentrates on regions where u_ε has to go above a given threshold. Then we restrict ourselves to the one-dimensional case and we show, more precisely, that the support of this energy is finite and concentrated where u_ε reaches the $1/4$ phase. We then consider in higher dimension the radially symmetric case. In all dimensions, the proposed analysis explains why the profile $y(s) = -q'(s)$ is well stabilized thanks to the Willmore term.

Section 3 focuses on the numerical discretization of the gradient flow of \mathcal{E}_ε , and in particular on its ability to approximate the mean curvature flow of non oriented interfaces. We illustrate this with various numerical simulations in dimensions 2 and 3.

2. CONVERGENCE ANALYSIS

We consider the functional $\mathcal{E}_\varepsilon(\cdot, Q)$ defined on $L^2(Q)$ as

$$\mathcal{E}_\varepsilon(u, Q) = \begin{cases} \int_Q \mathbf{m}_\varepsilon(u) dx + \frac{\sigma_\varepsilon}{2\varepsilon} \int_Q \mathbf{eul}_\varepsilon(u)^2 dx & \text{if } u \in W^{2,2}(Q), \ 0 \leq u \leq \frac{1}{4} \text{ a.e.}, \\ +\infty & \text{otherwise,} \end{cases}$$

with

$$\mathbf{m}_\varepsilon(u) = \frac{\varepsilon}{2} |\nabla u|^2 + \frac{1}{\varepsilon} F(u) \quad \text{and} \quad \mathbf{eul}_\varepsilon(u) = -\varepsilon \Delta u + \frac{1}{\varepsilon} F'(u).$$

As explained previously, although this phase field model seems very close to approximation models for the area plus Willmore energy involving a quadratic potential $W(s) = \frac{1}{2}s^2(1-s)^2$, the analysis here is very different because of the particular choice of F which admits an obstacle and not a double well in $s = 1/4$. The first difficulty is that any minimizing sequence $(u_\varepsilon)_\varepsilon$ of \mathcal{E}_ε converges a.e. to 0, hence does not allow us, in contrast with the classical Cahn-Hilliard approximation, to identify as the boundary of a limit domain a limit set Γ where the area plus Willmore energy concentrates. Intuitively, this follows from F having a non vanishing derivative at $s = 1/4$, making the phase $\{s = 1/4\}$ unstable. An alternative to identify the limit set is to consider the support of the limit measure of diffuse perimeter measures.

Given a sequence $(u_\varepsilon)_\varepsilon$ satisfying $\mathcal{E}_\varepsilon(u_\varepsilon, Q) \leq C < +\infty$, we define as in [28, 48, 50, 51] the absolutely continuous measures

$$\mu_\varepsilon = \left(\frac{\varepsilon}{2} |\nabla u_\varepsilon|^2 + \frac{1}{\varepsilon} F(u_\varepsilon) \right) \mathcal{L}^d.$$

There exists a Radon measure μ such that, possibly passing to a subsequence,

$$\mu_\varepsilon \text{ converges weakly-}^* \text{ to } \mu \text{ as } \varepsilon \rightarrow 0.$$

We study hereafter the properties of the support of μ and its relationship with the limit of $\mathcal{E}_\varepsilon(u_\varepsilon, Q)$. We consider first the problem in dimension $d = 1$, then the radially symmetric case in higher dimensions.

2.1. Control of the bulk energy. A first result, strongly inspired by [6, 28], consists in showing, thanks to the contribution of the Willmore term, that in the neighborhood of the support of μ , u_ε does indeed involve a diffuse interface. More precisely, we prove that for any z_0 in the support of μ , there exists for some fixed $\eta > 0$ a subsequence $x_\varepsilon \rightarrow 0$ such that $u_\varepsilon(x_\varepsilon) > \eta$.

Lemma 2.1. *Let $(u_\varepsilon)_\varepsilon$ be a sequence of functions in $W^{2,2}(\mathbb{R}^d)$ such that $\mathcal{E}_\varepsilon(u_\varepsilon, \mathbb{R}^d) \leq C < +\infty$ and $\mu_\varepsilon = \left(\frac{\varepsilon}{2} |\nabla u_\varepsilon|^2 + \frac{1}{\varepsilon} F(u_\varepsilon) \right) \mathcal{L}^d$ converges weakly- * to a Radon measure μ as $\varepsilon \rightarrow 0^+$. Let $z_0 \in \text{spt}(\mu)$, $r > 0$ and $\eta \in [0, \eta_0/2]$ where $\eta_0 = 1/12$. Then there exists $\bar{\varepsilon}$ such that*

$$B_r(z_0) \cap \{u_\varepsilon > \eta\} \neq \emptyset, \quad \forall \varepsilon \in]0, \bar{\varepsilon}[.$$

Proof. The proof is a minor modification of the proof of Lemma 4.4 in [6] adapted to our potential F . We exploit some properties of F , in particular that $F''(s) = 1 - 12s \geq 0$ for all $s \leq \eta_0 = 1/12$ as well as the existence of $c > 0$ such as $F(s) \leq cF'(s)^2$ for all $s \leq \eta_0/2$.

Let A_1, A_2 be two open subsets of \mathbb{R}^d with $A_1 \subset\subset A_2 \subset\subset \mathbb{R}^d$. Let us prove that there exists a positive constant C_0 such that

$$\begin{aligned} \int_{A_1 \cap \{u_\varepsilon \leq \eta\}} [\mathbf{m}_\varepsilon(u_\varepsilon) + \frac{1}{\varepsilon} F'(u_\varepsilon)^2] dx &\leq C_0 \eta \int_{A_2 \cap \{u_\varepsilon > \eta\}} [\varepsilon |\nabla u_\varepsilon|^2] dx + C_0 \varepsilon \int_{\mathbb{R}^d} (\mathbf{eul}_\varepsilon(u_\varepsilon))^2 dz \\ &+ C_0 \varepsilon^{1/2} \left[\int_{\mathbb{R}^d} \mathbf{m}_\varepsilon(u_\varepsilon) dx \right]^{1/2}, \end{aligned}$$

for ε sufficiently small.

Let $\phi \in C_c^\infty(A_2; [0, 1])$ be such that $\phi = 1$ on A_1 . Consider the function g defined by $g(s) = F'(s)$ for all $s \leq \eta$, $g(s) = 0$ for all $s > \frac{1}{12}$ and g affine on $[\eta, \frac{1}{12}]$. In particular, $g'(s) < 0$ for $\eta < s < \frac{1}{12}$, and $0 \leq g^2(s) \leq F'(s)g(s)$ for all $s \in \mathbb{R}$. Using the identity

$$\int_{\mathbb{R}^d} \phi \mathbf{eul}_\varepsilon(u_\varepsilon) g(u_\varepsilon) dx = \int_{\mathbb{R}^d} \left[\varepsilon g'(u_\varepsilon) |\nabla u_\varepsilon|^2 \phi + \frac{1}{\varepsilon} F'(u_\varepsilon) g(u_\varepsilon) \phi + \varepsilon g(u_\varepsilon) \nabla u_\varepsilon \cdot \nabla \phi \right] dx,$$

and observing that

$$\begin{aligned} \int_{\mathbb{R}^d} \phi \mathbf{eul}_\varepsilon(u_\varepsilon) g(u_\varepsilon) dx &\leq \int_{\mathbb{R}^d} \frac{1}{2} \phi \left[\varepsilon \mathbf{eul}_\varepsilon(u_\varepsilon)^2 + \frac{1}{\varepsilon} g(u_\varepsilon)^2 \right] dx \\ &\leq \int_{\mathbb{R}^d} \frac{1}{2} \phi \left[\varepsilon \mathbf{eul}_\varepsilon(u_\varepsilon)^2 + \frac{1}{\varepsilon} F'(u_\varepsilon) g(u_\varepsilon) \right] dx, \end{aligned}$$

we obtain that

$$\int_{\mathbb{R}^d} \phi [\varepsilon g'(u_\varepsilon) |\nabla u_\varepsilon|^2] dx \leq \int_{\mathbb{R}^d} \phi \frac{1}{2} \left[\varepsilon \mathbf{eul}_\varepsilon(u)^2 - \frac{1}{\varepsilon} F'(u_\varepsilon) g(u_\varepsilon) \right] dx - \int_{\mathbb{R}^d} \varepsilon g(u_\varepsilon) \nabla u_\varepsilon \cdot \nabla \phi dx.$$

Then,

$$\begin{aligned}
& \int_{\{u_\varepsilon \leq \eta\} \cap A_1} \left[\varepsilon F''(u_\varepsilon) |\nabla u_\varepsilon|^2 + \frac{1}{2\varepsilon} F'(u_\varepsilon)^2 \right] dx \leq \int_{\{u_\varepsilon \leq \eta\}} \phi \left[\varepsilon g'(u_\varepsilon) |\nabla u_\varepsilon|^2 + \frac{1}{2\varepsilon} F'(u_\varepsilon) g(u_\varepsilon) \right] dx \\
& \leq \frac{\varepsilon}{2} \int_{\mathbb{R}^d} \mathbf{eul}_\varepsilon(u_\varepsilon)^2 dx - \int_{\{u_\varepsilon > \eta\}} \phi \left[\varepsilon g'(u_\varepsilon) |\nabla u_\varepsilon|^2 \right] - \int_{\mathbb{R}^d} \varepsilon g(u_\varepsilon) \nabla u_\varepsilon \cdot \nabla \phi dx, \\
& \leq \frac{\varepsilon}{2} \int_{\mathbb{R}^d} \mathbf{eul}_\varepsilon(u_\varepsilon)^2 dx - \int_{\{u_\varepsilon > \eta\} \cap A_2} \left[\varepsilon g'(u_\varepsilon) |\nabla u_\varepsilon|^2 \right] + \left| \int_{A_2} \varepsilon g(u_\varepsilon) \nabla u_\varepsilon \cdot \nabla \phi dx \right|.
\end{aligned}$$

Using Hölder's inequality, we obtain that there exists a constant C depending on A_2 , ϕ and F such that

$$\begin{aligned}
\left| \int_{A_2} \varepsilon g(u_\varepsilon) \nabla u_\varepsilon \cdot \nabla \phi dx \right| & \leq \varepsilon^{1/2} \|\nabla \phi\|_\infty \sup_{[0, 1/4]} |g| |A_2 \setminus A_1|^{1/2} \left[\int_{\mathbb{R}^d} \varepsilon |\nabla u_\varepsilon|^2 dx \right]^{1/2} \\
& \leq C \varepsilon^{1/2} \left[\int_{\mathbb{R}^d} \mathbf{m}_\varepsilon(u_\varepsilon) dx \right]^{1/2}.
\end{aligned}$$

Finally, as for all $s < \eta$ $F''(s) \geq c_0$ and $F(s) \leq c_1 F'(s)^2$, we deduce that there exists $C > 0$ such that

$$\int_{A_1 \cap \{u_\varepsilon \leq \eta\}} \left[\mathbf{m}_\varepsilon(u_\varepsilon) + \frac{1}{\varepsilon} F'(u_\varepsilon)^2 \right] dx \leq C \int_{\{u_\varepsilon \leq \eta\} \cap A_1} \left[\varepsilon F''(u_\varepsilon) |\nabla u_\varepsilon|^2 + \frac{1}{2\varepsilon} F'(u_\varepsilon)^2 \right] dx.$$

Moreover, as there exists $c > 0$ such that $|g'(s)| \leq c\eta$ for all $s \in [\eta, 1/12]$, we deduce the existence of $C_0 > 0$ such that

$$\begin{aligned}
\int_{A_1 \cap \{u_\varepsilon \leq \eta\}} \left[\mathbf{m}_\varepsilon(u_\varepsilon) + \frac{1}{\varepsilon} F'(u_\varepsilon)^2 \right] dx & \leq C_0 \eta \int_{A_2 \cap \{u_\varepsilon > \eta\}} [\varepsilon |\nabla u_\varepsilon|^2] dx + C_0 \varepsilon \int_{\mathbb{R}^d} (\mathbf{eul}_\varepsilon(u_\varepsilon))^2 dx \\
& + C_0 \varepsilon^{1/2} \left[\int_{\mathbb{R}^d} \mathbf{m}_\varepsilon(u_\varepsilon) dx \right]^{1/2}.
\end{aligned}$$

We can now complete the proof of the lemma. Suppose by contradiction that there exists a decreasing sequence ε such that $B_r(z_0) \subseteq \{u_\varepsilon < \eta\}$. Using $A_1 = B_{r/2}(z_0)$ and $A_2 = B_r(z_0)$, thus $\{u_\varepsilon > \eta\} \cap A_2 = \emptyset$, it follows that

$$\begin{aligned}
0 < \mu(B_{r/2}(z_0)) & \leq \liminf_{\varepsilon \rightarrow 0} \int_{A_1 \cap \{u_\varepsilon \leq \eta\}} \mathbf{m}_\varepsilon(u_\varepsilon) dx \\
& \leq C_0 \lim_{\varepsilon \rightarrow 0} \varepsilon \int_{\mathbb{R}^d} (\mathbf{eul}_\varepsilon(u_\varepsilon))^2 dx + \varepsilon^{1/2} \left[\int_{\mathbb{R}^d} \mathbf{m}_\varepsilon(u_\varepsilon) dx \right]^{1/2} = 0,
\end{aligned}$$

hence the contradiction. \square

2.2. Limit phase and limit energy measure: the one-dimensional case. In dimension one, the Willmore term does not give an explicit contribution to the lower bound of the limit energy measure exhibited in the next theorem. But the term is crucial to guarantee the stability of the profile function q' .

For every $\varepsilon > 0$, the one-dimensional energy \mathcal{E}_ε of defined for all $u \in W^{2,2}([a, b])$ as:

$$\mathcal{E}_\varepsilon(u, (a, b)) = \begin{cases} \int_a^b \left(\frac{\varepsilon}{2} |u'|^2 + \frac{1}{\varepsilon} F(u) \right) dx + \frac{\sigma_\varepsilon}{2\varepsilon} \int_a^b \left(\varepsilon u'' - \frac{1}{\varepsilon} F'(u) \right)^2 dx & \text{if } 0 \leq u \leq \frac{1}{4} \text{ a.e.}, \\ +\infty & \text{otherwise.} \end{cases}$$

where σ_ε is a positive function of ε and $\sigma_\varepsilon \rightarrow \sigma_0 \geq 0$ as $\varepsilon \rightarrow 0$.

Theorem 2.2. Assume that $\varepsilon^2/\sigma_\varepsilon \rightarrow 0$ as $\varepsilon \rightarrow 0^+$, and let $(u_\varepsilon)_\varepsilon$ be a sequence such that, for all $\varepsilon > 0$, $\mathcal{E}_\varepsilon(u_\varepsilon) \leq C$ with $C > 0$ and such that $\mu_\varepsilon := (\frac{\varepsilon}{2}|\nabla u_\varepsilon|^2 + \frac{1}{\varepsilon}F(u_\varepsilon))\mathcal{L}^d$ converges weakly-* to a Radon measure μ as $\varepsilon \rightarrow 0$. We let $c_F := 2 \int_0^{1/4} \sqrt{2F(t)}dt = 1/60$. Then

- (u_ε) converges a.e. to $u \equiv 0$.
- The support of μ is a finite collection $\{x_i\}_{i \in I}$ of points.
- For ε small enough, $u_\varepsilon \approx 1/4$ near every x_i .
- $\mu \geq c_F \sum_i \delta_{x_i}$

Proof. Since $\mathcal{E}_\varepsilon(u_\varepsilon) \leq C < +\infty$, we have $\int_a^b F(u_\varepsilon)dx \leq C\varepsilon$ and $\int_a^b \sqrt{2F(u_\varepsilon)}|u'_\varepsilon|dx \leq C$. This shows that $w_\varepsilon(x) := \int_0^{u_\varepsilon(x)} \sqrt{2F(t)}dt$ is bounded in $BV(a, b)$. Remark that, for all ε , $u_\varepsilon \in C^1$ by Sobolev injection theorem. Possibly passing to a subsequence, we may assume that (w_ε) converges in $L^1(a, b)$ (or any $L^p(a, b)$, $p < +\infty$) and a.e., so that also (u_ε) converges a.e. to some limit function u . Because $\int_a^b F(u_\varepsilon)dx \rightarrow 0$ we get that $F(u(x)) = 0$ a.e., so $u(x) \in \{0, \frac{1}{4}\}$ for a.e. x .

For $\delta \in (0, 1/4)$, let

$$I_\delta := \left\{ x \in (a, b) : \exists x_\varepsilon \rightarrow x, \limsup_\varepsilon u_\varepsilon(x_\varepsilon) \geq \delta \right\}$$

It follows from Lemma 2.1 in the previous section that $\text{spt}(\mu) \subset I_\delta$ for $\delta > 0$ small enough.

We divide the proof into several steps.

Step #1: we prove that, for all $\delta > 0$, $I_\delta = I_{1/4}$, and that $u_\varepsilon \approx 1/4$ near every x_i for ε small enough.

Let $\bar{x} \in I_\delta$. From now on, we consider further subsequences which possibly depend on \bar{x} . We first consider $x_\varepsilon \rightarrow \bar{x}$ such that $\lim_\varepsilon u_\varepsilon(x_\varepsilon) \geq \delta$.

Let $\eta > 0$. We first show that $\max_{[\bar{x}-\eta, \bar{x}+\eta]} u_\varepsilon \rightarrow 1/4$ as $\varepsilon \rightarrow 0$. Assume without loss of generality that $u_\varepsilon(\bar{x} \pm \eta)$ converge to some value in $\{0, 1/4\}$ as $\varepsilon \rightarrow 0$, since this is true for a.e. $\eta > 0$. If one of the limits is $1/4$, there is nothing to prove, so we assume that $u_\varepsilon(\bar{x} \pm \eta) \rightarrow 0$. We introduce the following functions v_ε involving a rescaling around x_ε :

$$v_\varepsilon(y) := u_\varepsilon(\varepsilon y + x_\varepsilon), \quad \frac{\bar{x} - x_\varepsilon - \eta}{\varepsilon} =: \alpha_\varepsilon \leq y \leq \beta_\varepsilon := \frac{\bar{x} - x_\varepsilon + \eta}{\varepsilon}.$$

Observe that, as $\varepsilon \rightarrow 0^+$, $\lim v_\varepsilon(0) \geq \delta$, $\alpha_\varepsilon \rightarrow -\infty$, $\beta_\varepsilon \rightarrow +\infty$, and $\lim v_\varepsilon(\alpha_\varepsilon) = \lim v_\varepsilon(\beta_\varepsilon) = 0$.

Since

$$C \geq \mathcal{E}_\varepsilon(u_\varepsilon, (\bar{x} - \eta, \bar{x} + \eta)) = \int_{\alpha_\varepsilon}^{\beta_\varepsilon} \frac{\sigma_\varepsilon}{2\varepsilon^2} (v_\varepsilon'' - F'(v_\varepsilon))^2 + \frac{|v_\varepsilon'|^2}{2} + F(v_\varepsilon)dy,$$

it follows, in particular, that $\mathbf{e}_\varepsilon := v_\varepsilon'' - F'(v_\varepsilon)$ satisfies

$$\int_{\alpha_\varepsilon}^{\beta_\varepsilon} \mathbf{e}_\varepsilon^2 dy \leq C \frac{2\varepsilon^2}{\sigma_\varepsilon} \rightarrow 0.$$

We deduce from the Cauchy-Schwarz inequality and the two inequalities above that

$$\int_{\alpha_\varepsilon}^{\beta_\varepsilon} |\mathbf{e}_\varepsilon v_\varepsilon'| dy \rightarrow 0.$$

For all x, t such that $\alpha_\varepsilon < t < 0 \leq x \leq \beta_\varepsilon$, and since $(\frac{1}{2}(v'_\varepsilon)^2 - F(v_\varepsilon))' = \mathbf{e}_\varepsilon v'_\varepsilon$, we have that

$$\left| \frac{v'_\varepsilon(x)^2}{2} - F(v_\varepsilon(x)) \right| = \left| \frac{v'_\varepsilon(t)^2}{2} - F(v_\varepsilon(t)) + \int_t^x \mathbf{e}_\varepsilon v'_\varepsilon dy \right| \leq \frac{v'_\varepsilon(t)^2}{2} + F(v_\varepsilon(t)) + \int_{\alpha_\varepsilon}^{\beta_\varepsilon} |\mathbf{e}_\varepsilon v'_\varepsilon| dy$$

Averaging this for $t \in (\alpha_\varepsilon, 0)$, we get

$$\left| \frac{v'_\varepsilon(x)^2}{2} - F(v_\varepsilon(x)) \right| \leq \frac{1}{-\alpha_\varepsilon} C + \int_{\alpha_\varepsilon}^{\beta_\varepsilon} |\mathbf{e}_\varepsilon v'_\varepsilon| dy \rightarrow 0$$

showing that $|v'_\varepsilon| - \sqrt{2F(v_\varepsilon)} \rightarrow 0$ uniformly in every compact of $[0, \infty)$. A similar computation, this time choosing $\alpha_\varepsilon < x \leq 0$ and integrating up to $t > 0, t < \beta_\varepsilon$, shows that the convergence is also uniform in every compact of $(-\infty, 0]$.

Consider now y_ε where $\max_{[\alpha_\varepsilon, \beta_\varepsilon]} v_\varepsilon$ is reached. It follows from the assumptions that, for ε small enough, y_ε is not on the boundary of $[\alpha_\varepsilon, \beta_\varepsilon]$ and $v_\varepsilon(y_\varepsilon) \geq \delta/2$. The function v_ε being smooth and y_ε not on the boundary, we have $v'_\varepsilon(y_\varepsilon) = 0$. As $|v'_\varepsilon| - \sqrt{2F(v_\varepsilon)} \rightarrow 0$ locally uniformly, we deduce that $\sqrt{2F(v_\varepsilon(y_\varepsilon))} \rightarrow 0$, hence $v_\varepsilon(y_\varepsilon) \rightarrow 1/4$ (as it cannot converge to 0 by definition of y_ε).

Returning back to the function u_ε on the interval $(\bar{x} - \eta, \bar{x} + \eta)$, we have proved that there exists x'_ε in this interval such that $u_\varepsilon(x'_\varepsilon) \rightarrow 1/4$. Finally, since η is arbitrary, we may build $x''_\varepsilon \rightarrow \bar{x}$ with $u_\varepsilon(x''_\varepsilon) \rightarrow 1/4$, showing that $\bar{x} \in I_{1/4}$. Hence, as claimed, $I_\delta = I_{1/4}$ for any $\delta > 0$. In addition, u_ε being smooth for all ε , we have $u_\varepsilon \approx \frac{1}{4}$ near every point of $I_{\frac{1}{4}}$ (the approximation being sharper as ε becomes smaller).

Step #2: we prove that $\text{spt } \mu \subset I_{1/4}$, that $I_{1/4}$ is a finite collection $\{x_i\}_{i \in I}$ of points, and that $u = 0$ a.e.

Let $\bar{x} \in I_{1/4}$. As before, we will assume that either the maximum of v_ε is reached on the boundary of $(\alpha_\varepsilon, \beta_\varepsilon)$, or $\lim_\varepsilon v_\varepsilon(\alpha_\varepsilon) = \lim_\varepsilon v_\varepsilon(\beta_\varepsilon) = 0$, in which case the maximum is reached inside the interval $(\alpha_\varepsilon, \beta_\varepsilon)$.

First we assume that the maximal value $v_\varepsilon(y_\varepsilon)$ is reached at $y_\varepsilon = \alpha_\varepsilon$ or β_ε . Assuming $y_\varepsilon \leq 0$ (the case $y_\varepsilon \geq 0$ is treated identically), we have $v'_\varepsilon(y_\varepsilon) \leq 0$ and for $t > y_\varepsilon$ one can write:

$$v'_\varepsilon(t) = v'_\varepsilon(y_\varepsilon) + \int_{y_\varepsilon}^t v''_\varepsilon(y) dy \leq \int_{y_\varepsilon}^t F'(v_\varepsilon(y)) dy + \int_{y_\varepsilon}^t \mathbf{e}_\varepsilon dy \leq \int_{y_\varepsilon}^t F'(v_\varepsilon(y)) dy + \sqrt{t - y_\varepsilon} \sqrt{C} \frac{\varepsilon}{\sqrt{\sigma_\varepsilon}}.$$

Integrating once more,

$$v_\varepsilon(t) \leq v_\varepsilon(y_\varepsilon) + \int_{y_\varepsilon}^t (t - y) F'(v_\varepsilon(y)) dy + \frac{2}{3} (t - y_\varepsilon)^{3/2} \sqrt{C} \frac{\varepsilon}{\sqrt{\sigma_\varepsilon}}.$$

Using in addition that $v_\varepsilon(t) \geq v_\varepsilon(y_\varepsilon) - \sqrt{2C} \sqrt{t - y_\varepsilon} = 1/4 - \sqrt{2C} \sqrt{t - y_\varepsilon} + o(1)$, we have $v_\varepsilon(t) \geq 1/5$ for $t \leq y'_\varepsilon = y_\varepsilon + 1/(800C) + o(1)$, and in particular $F'(v_\varepsilon(t)) \leq F'(1/5) < 0$. Hence,

$$v_\varepsilon(y'_\varepsilon) \leq v_\varepsilon(y_\varepsilon) + F'(1/5) \frac{(y'_\varepsilon - y_\varepsilon)^2}{2} + \frac{2}{3} (y'_\varepsilon - y_\varepsilon)^{3/2} \sqrt{C} \frac{\varepsilon}{\sqrt{\sigma_\varepsilon}} \rightarrow \frac{1}{4} - \frac{|F'(1/5)|}{2} \frac{1}{(800C)^2} =: \bar{v}$$

as $\varepsilon \rightarrow 0$. We then deduce that

$$\mathcal{E}_\varepsilon(u_\varepsilon, (\bar{x} - \eta, \bar{x} + \eta)) \geq \int_{\bar{v}}^{1/4} \sqrt{2F(t)} dt \geq c_{\bar{v}} > 0.$$

We now consider the other situation, i.e. when $u_\varepsilon(\bar{x} \pm \eta) \rightarrow 0$. We recall that

$$\begin{aligned} \mathcal{E}_\varepsilon(u_\varepsilon, (\bar{x} - \eta, \bar{x} + \eta)) &= \int_{\alpha_\varepsilon}^{y_\varepsilon} \frac{\sigma_\varepsilon}{2\varepsilon^2} (v_\varepsilon'' - F'(v_\varepsilon))^2 + \frac{|v_\varepsilon'|^2}{2} + F(v_\varepsilon) dy \\ &\quad + \int_{y_\varepsilon}^{\beta_\varepsilon} \frac{\sigma_\varepsilon}{2\varepsilon^2} (v_\varepsilon'' - F'(v_\varepsilon))^2 + \frac{|v_\varepsilon'|^2}{2} + F(v_\varepsilon) dy, \end{aligned}$$

and we observe that

$$\begin{aligned} \int_{\alpha_\varepsilon}^{y_\varepsilon} \left(\frac{\sigma_\varepsilon}{2\varepsilon^2} (v_\varepsilon'' - F'(v_\varepsilon))^2 + \frac{|v_\varepsilon'|^2}{2} + F(v_\varepsilon) \right) dy &\geq \int_{\alpha_\varepsilon}^{y_\varepsilon} \left(\frac{|v_\varepsilon'|^2}{2} + F(v_\varepsilon) \right) dy \\ &\geq \int_{\alpha_\varepsilon}^{y_\varepsilon} \sqrt{2F(v_\varepsilon)} |v_\varepsilon'| dy \geq \int_{v(\alpha_\varepsilon)}^{v(y_\varepsilon)} \sqrt{2F(s)} ds \rightarrow \int_0^{1/4} \sqrt{2F(s)} ds, \end{aligned}$$

Arguing similarly for the second integral yields finally

$$\liminf_{\varepsilon \rightarrow 0} \mathcal{E}_\varepsilon(u_\varepsilon, (\bar{x} - \eta, \bar{x} + \eta)) \geq \liminf_{\varepsilon \rightarrow 0} \mu_\varepsilon(u_\varepsilon, (\bar{x} - \eta, \bar{x} + \eta)) \geq 2 \int_0^{1/4} \sqrt{2F(s)} ds =: c_F.$$

We find that in both cases the energy in the interval $(\bar{x} - \eta, \bar{x} + \eta)$ is bounded from below by a constant, and since η is arbitrarily small, we deduce that $I_{\frac{1}{4}}$ is a finite collection $\{x_i\}_{i \in I}$ of points, hence $u = 0$ almost everywhere. As $\text{spt}(\mu) \subset I_\delta$ for δ small enough and $I_\delta = I_{\frac{1}{4}}$ for all δ , we conclude that $\text{spt}(\mu) \subset \bigcup_{i \in I} \{x_i\}$.

Step #3: we prove that $\text{spt} \mu = I_{\frac{1}{4}} = \bigcup_{i \in I} \{x_i\}$ and we identify a lower bound for μ .

We know that $\text{spt}(\mu) \subset I_{\frac{1}{4}}$. Since $u = 0$ a.e., we can choose η above so that $u_\varepsilon(\bar{x} \pm \eta) \rightarrow 0$ as $\varepsilon \rightarrow 0$ (by definition of $I_{\frac{1}{4}}$, we also have that $u_\varepsilon \rightarrow 0$ locally uniformly in $(a, b) \setminus I_{1/4}$). We deduce from the inequality

$$\liminf_{\varepsilon \rightarrow 0} \mathcal{E}_\varepsilon(u_\varepsilon, (\bar{x} - \eta, \bar{x} + \eta)) \geq \liminf_{\varepsilon \rightarrow 0} \mu_\varepsilon(u_\varepsilon, (\bar{x} - \eta, \bar{x} + \eta)) \geq 2 \int_0^{1/4} \sqrt{2F(s)} ds =: c_F.$$

proved above that $\mu(\bar{x} - \eta, \bar{x} + \eta) \geq c_F$ for any $\eta > 0$, thus

$$\mu \geq c_F \mathcal{H}^0 \llcorner I_{\frac{1}{4}}.$$

It follows in particular that $\text{spt} \mu = I_{\frac{1}{4}} = \bigcup_{i \in I} \{x_i\}$. \square

Remark 2.3. It is a consequence of the Γ -lim sup result that we will state later in any dimension that the energy inequality proved in the previous theorem is optimal.

Remark 2.4. We now provide an example showing that the limit energy can reach, locally, any value above c_F . Recall first that $\xi = -q'$ is a solution to the equations $\xi'' = F'(\xi)$ and $|\xi'| = \sqrt{2F(\xi)}$. However, since $\sqrt{2F}$ is not Lipschitz at $x = 1/4$, it follows that $\xi = -q'$ is not the only solution to the constrained problem

$$\begin{aligned} |\xi'(s)| &= \sqrt{2F(\xi(s))}, \quad s \in \mathbb{R} \\ \xi(0) &= \frac{1}{4}, \quad \lim_{s \rightarrow \pm\infty} \xi(s) = 0. \end{aligned}$$

In particular, for all $c > 0$, the function ξ_c defined by

$$\xi_c(s) = \begin{cases} 1/4 & \text{if } |s| \leq c \\ -q'(s - c) & \text{if } s > c \\ -q'(s + c) & \text{if } s < -c \end{cases}$$

is another solution.

Let us now consider the sequence $\{u_\varepsilon\}_\varepsilon$ defined by $u_\varepsilon(x) = \xi_{d_\varepsilon}(x/\varepsilon)$ where $d_\varepsilon > 0$ will be chosen later. It is not difficult to see that

$$\int_{\mathbb{R}} \varepsilon \left(\frac{|u'_\varepsilon(x)|^2}{2} + \frac{1}{\varepsilon} F(u_\varepsilon(x)) \right) dx = c_F$$

and

$$\frac{\sigma_\varepsilon}{2\varepsilon} \int_{\mathbb{R}} \left(\varepsilon u''_\varepsilon(x) - \frac{1}{\varepsilon} F'(u_\varepsilon(x)) \right)^2 dx = \frac{\sigma_\varepsilon d_\varepsilon}{2\varepsilon^2} F'(1/4)^2.$$

For any $\theta > 0$, we define $d_\varepsilon = \frac{2\theta\varepsilon^2}{\sigma_\varepsilon}$ and we observe that $\lim_{\varepsilon \rightarrow 0} d_\varepsilon = 0$. We obtain that

$$\lim_{\varepsilon \rightarrow 0} \mathcal{E}_\varepsilon(u_\varepsilon) = c_F + \theta F'(1/4)^2.$$

As θ is arbitrary and $F'(1/4) \neq 0$, we conclude that the limit mass can actually reach, locally, any value above c_F . This example shows, in addition, that the Willmore term in the approximating energy does not always contribute explicitly to the limit energy in dimension 1, in contrast with the higher-dimensional case that we study in the next section.

2.3. Limit phase and limit energy measure: the radially symmetric case in dimension $d \geq 2$.

We now consider the problem in \mathbb{R}^d , $d \geq 2$, looking only at radially symmetric functions. The analysis is very similar to the 1D case, it shows in addition that the Willmore approximation term not only stabilizes the profile q' but also contributes explicitly in the limit to the energy of the limit support.

For $u \in W^{2,2}(Q)$, we consider

$$\mathcal{E}_\varepsilon(u, Q) = \begin{cases} \int_Q \mathbf{m}_\varepsilon(u) dx + \frac{\sigma_\varepsilon}{2\varepsilon} \int_Q [\mathbf{eul}_\varepsilon(u)]^2 dx & \text{if } 0 \leq u \leq \frac{1}{4} \text{ a.e.}, \\ +\infty & \text{otherwise,} \end{cases}$$

where $\sigma_\varepsilon > 0$, $\sigma_\varepsilon \rightarrow \sigma_0 \geq 0$ as $\varepsilon \rightarrow 0$, and

$$\begin{aligned} \mathbf{m}_\varepsilon(u) &= \frac{\varepsilon}{2} |\nabla u|^2 + \frac{1}{\varepsilon} F(u) \\ \mathbf{eul}_\varepsilon(u) &= \varepsilon \Delta u - \frac{1}{\varepsilon} F'(u). \end{aligned}$$

Theorem 2.5. *Let $R > 0$ be such that $B_R \subset Q$. Let $(u_\varepsilon)_\varepsilon$ be a sequence of radially symmetric functions in $W^{2,2}(Q)$ such that $\mathcal{E}_\varepsilon(u_\varepsilon, B_R) \leq C < +\infty$. Assume that $\lim_{\varepsilon \rightarrow 0^+} \sigma_\varepsilon = \sigma_0 \geq 0$ and $\lim_{\varepsilon \rightarrow 0^+} \varepsilon^2/\sigma_\varepsilon \rightarrow 0$. Possibly taking a subsequence, we assume that there exist two Radon measures μ, ξ such that, as $\varepsilon \rightarrow 0^+$, $\mu_\varepsilon := \mathbf{m}_\varepsilon(u_\varepsilon) \mathcal{L}^d$ converges weakly-* to μ and $\xi_\varepsilon := (\mathbf{m}_\varepsilon(u_\varepsilon) + \frac{\sigma_\varepsilon}{2\varepsilon} [\mathbf{eul}_\varepsilon(u_\varepsilon)]^2) \mathcal{L}^d$ converges weakly-* to ξ . Then, outside of an arbitrary small neighborhood of 0 and possibly passing to a subsequence,*

- (u_ε) converges a.e. to $u \equiv 0$.
- The support of μ is concentrated on a finite collection $\{\partial B(0, r_i), i \in I\}$ of $(d-1)$ -spheres centered at 0 (with $\text{card } I$ depending on the chosen neighborhood of 0).
- For ε small enough, $u_\varepsilon \approx 1/4$ near ∂B_{r_i} for all $i \in I$.
- The measure ξ satisfies outside the neighborhood of 0

$$\xi \geq c_F \sum_{i \in I} \left(1 + \sigma_0 \frac{(d-1)^2}{r_i^2} \right) \mathcal{H}^{d-1} \llcorner \partial B_{r_i},$$

$$\text{where } c_F = 2 \int_0^{1/4} \sqrt{2F(t)} dt = 1/60.$$

Observe that in case $\sigma_0 > 0$, the results hold in $(0, R)$ (without removing a neighborhood of 0).

Proof. We first prove that, possibly passing to a subsequence, for a.e. x $u_\varepsilon(x) \rightarrow u(x) \in \{0, \frac{1}{4}\}$. Indeed, as in the one-dimensional case, we have $\int_{B_R} F(u_\varepsilon) dx \leq C\varepsilon$ and $\int_{B_R} \sqrt{2F(u_\varepsilon)} |\nabla u_\varepsilon| dx \leq C$. This shows that $w_\varepsilon(x) := \int_0^{u_\varepsilon(x)} \sqrt{2F(t)} dt$ is bounded in $BV(B_R)$. Possibly passing to a subsequence, we may assume that (w_ε) converges in $L^1(B_R)$ (or any $L^p(B_R)$, $p < +\infty$) and almost everywhere, so that also (u_ε) converges a.e. to some limit function u . Because $\int_{B_R} F(u_\varepsilon) dx \rightarrow 0$ we get that $F(u) = 0$ a.e., therefore $u(x) \in \{0, \frac{1}{4}\}$ a.e.

Using the radial symmetry of u_ε , let us introduce $\bar{u}_\varepsilon : [0, R] \rightarrow \mathbb{R}$ such that, for all $x \in B_R$, $u_\varepsilon(x) = \bar{u}_\varepsilon(|x|)$. We define for $\delta \in (0, 1/4]$

$$I_\delta := \left\{ r \in \mathbb{R}_+^* : \exists r_\varepsilon > 0 \rightarrow r, \limsup_\varepsilon \bar{u}_\varepsilon(r_\varepsilon) \geq \delta \right\}$$

We divide the rest of the proof into several steps.

Step #1: we prove that $I_\delta = I_{1/4}$ for all $\delta > 0$.

The proof follows exactly the same arguments as in the one-dimensional case.

Let $\bar{r} \in I_\delta \setminus \{0\}$. Consider a positive sequence (r_ε) such that $r_\varepsilon \rightarrow \bar{r}$ and $\lim_{\varepsilon \rightarrow 0} \bar{u}_\varepsilon(r_\varepsilon) \geq \delta$. For a.e. $\eta > 0$, we will show that $\max_{[\bar{r}-\eta, \bar{r}+\eta]} \bar{u}_\varepsilon \rightarrow 1/4$ as $\varepsilon \rightarrow 0$. We first define

$$v_\varepsilon(y) := \bar{u}_\varepsilon(\varepsilon y + r_\varepsilon), \quad \text{with} \quad \frac{\bar{r} - r_\varepsilon - \eta}{\varepsilon} =: \alpha_\varepsilon \leq y \leq \beta_\varepsilon := \frac{\bar{r} - r_\varepsilon + \eta}{\varepsilon}.$$

As $u(x) \in \{0, \frac{1}{4}\}$ a.e., we can assume that $\bar{u}_\varepsilon(\bar{r} \pm \eta) \rightarrow \{0, \frac{1}{4}\}$. If $\bar{u}_\varepsilon(\bar{r} \pm \eta) \rightarrow \frac{1}{4}$ there is nothing more to prove, hence we assume that $\lim_\varepsilon v_\varepsilon(\alpha_\varepsilon) = \lim_\varepsilon v_\varepsilon(\beta_\varepsilon) = 0$. We let

$$T_{\eta, \bar{r}} = \{x \in B_R, |x| \in [\bar{r} - \eta, \bar{r} + \eta]\}$$

and we obtain that

$$(2.1) \quad \int_{T_{\eta, \bar{r}}} \mathbf{m}_\varepsilon(u_\varepsilon) dx = |S^{d-1}| r_\varepsilon^{d-1} \int_{\alpha_\varepsilon}^{\beta_\varepsilon} \left[\frac{|v'_\varepsilon|^2}{2} + F(v_\varepsilon) \right] |1 + \varepsilon y / r_\varepsilon|^{d-1} dy \leq C,$$

where $S^{d-1} = \{x \in \mathbb{R}^d, \|x\| = 1\}$ is the unit sphere. Moreover,

$$\frac{\sigma_\varepsilon}{\varepsilon} \int_{T_{\eta, \bar{r}}} \mathbf{eul}_\varepsilon(u_\varepsilon)^2 dx = |S^{d-1}| r_\varepsilon^{d-1} \frac{\sigma_\varepsilon}{\varepsilon^2} \int_{\alpha_\varepsilon}^{\beta_\varepsilon} \left[-v''_\varepsilon + F'(v_\varepsilon) + \frac{(d-1)\varepsilon/r_\varepsilon}{1 + \varepsilon y / r_\varepsilon} v'_\varepsilon \right]^2 |1 + \varepsilon y / r_\varepsilon|^{d-1} dy \leq C.$$

Since $\frac{\bar{r}-\eta}{r_\varepsilon} \leq 1 + \varepsilon y / r_\varepsilon \leq \frac{\bar{r}+\eta}{r_\varepsilon}$, we can assume that ε, η are enough small so that for all $y \in [\alpha_\varepsilon, \beta_\varepsilon]$,

$$(2.2) \quad \frac{1}{2} \leq |1 + \varepsilon y / r_\varepsilon| \leq \frac{3}{2}.$$

With $\mathbf{e}_\varepsilon := v''_\varepsilon - F'(v_\varepsilon)$ and $w_\varepsilon = \frac{(d-1)\varepsilon/r_\varepsilon}{1 + \varepsilon y / r_\varepsilon} v'_\varepsilon$, it follows that

$$|S^{d-1}| r_\varepsilon^{d-1} \int_{\alpha_\varepsilon}^{\beta_\varepsilon} |w_\varepsilon|^2 dy \leq C(\varepsilon/r_\varepsilon)^2.$$

Moreover, since

$$\begin{aligned} |S^{d-1}|r_\varepsilon^{d-1} \int_{\alpha_\varepsilon}^{\beta_\varepsilon} \mathbf{e}_\varepsilon^2 dy &\leq |S^{d-1}|r_\varepsilon^{d-1} \int_{\alpha_\varepsilon}^{\beta_\varepsilon} (\mathbf{e}_\varepsilon + w_\varepsilon)^2 - 2\mathbf{e}_\varepsilon w_\varepsilon dy \\ &\leq |S^{d-1}|r_\varepsilon^{d-1} \int_{\alpha_\varepsilon}^{\beta_\varepsilon} (\mathbf{e}_\varepsilon + w_\varepsilon)^2 + |S^{d-1}|r_\varepsilon^{d-1} \varepsilon \int_{\alpha_\varepsilon}^{\beta_\varepsilon} \mathbf{e}_\varepsilon^2 dy + C\varepsilon/r_\varepsilon^2, \end{aligned}$$

we obtain that

$$(2.3) \quad \int_{\alpha_\varepsilon}^{\beta_\varepsilon} \mathbf{e}_\varepsilon^2 dy \leq C \frac{1}{|S^{d-1}|r_\varepsilon^{d-1}(1-\varepsilon)} \left(\frac{\varepsilon^2}{\sigma_\varepsilon} + \frac{\varepsilon}{r_\varepsilon^2} \right) \rightarrow 0.$$

We deduce from (2.1), (2.2), (2.3), the assumption $r_\varepsilon \rightarrow \bar{r} \neq 0$ and the Cauchy-Schwarz inequality that

$$\int_{\alpha_\varepsilon}^{\beta_\varepsilon} |\mathbf{e}_\varepsilon v'_\varepsilon| dy \rightarrow 0.$$

Using $\left(\frac{(v'_\varepsilon)^2}{2} - F(v_\varepsilon) \right)' = \mathbf{e}_\varepsilon v'_\varepsilon$, the rest of the proof of Step #1 is based on the very same arguments as in the one-dimensional case, and we conclude that $|v'_\varepsilon| - \sqrt{2F(v_\varepsilon)} \rightarrow 0$ locally uniformly, that the maximum of v_ε is reached at y_ε , which satisfies $v_\varepsilon(y_\varepsilon) \rightarrow 1/4$, and, finally, that $I_\delta = I_{1/4}$ for all $\delta > 0$.

Step #2: $I_{1/4}$ hence $\text{spt } \mu$ are concentrated on a finite collection of $(d-1)$ -spheres (centered at 0) outside the chosen neighborhood of 0.

The proof is almost identical to the one-dimensional case. We have the following two situations, depending on whether the maximum of v_ε is reached at the boundary or inside the interval $[\alpha_\varepsilon, \beta_\varepsilon]$. In the first case, we can deduce the existence of $\bar{v} < 1/4$ such that

$$\lim_{\varepsilon \rightarrow 0^+} \int_{T_{\eta, \bar{r}}} \mathbf{m}_\varepsilon(u_\varepsilon) dx \geq |S^{d-1}|\bar{r}^{d-1} \int_{\bar{v}}^{1/4} \sqrt{2F(t)} dt > 0.$$

In the second case, as for ε small enough we have that $1 - \eta_\varepsilon \leq |1 + \varepsilon y/r_\varepsilon| \leq 1 + \eta_\varepsilon$ with $\eta_\varepsilon \rightarrow \frac{\eta}{\bar{r}}$, we deduce that

$$\liminf_{\varepsilon \rightarrow 0^+} \int_{T_{\eta, \bar{r}}} \mathbf{m}_\varepsilon(u_\varepsilon) dx \geq |S^{d-1}|\bar{r}^{d-1} \left(1 - \frac{\eta}{\bar{r}}\right)^{d-1} c_F > 0.$$

Since $\mathcal{L}^d(T_{\eta, \bar{r}}) \rightarrow 0$ as $\eta \rightarrow 0$ and $\partial B(0, \bar{r}) \subset T_{\eta, \bar{r}}$ for all η , we deduce in both cases above that, outside any neighborhood of 0, $I_{1/4}$ is concentrated on a finite collection of $(d-1)$ -spheres centered at 0, therefore $u = 0$ almost everywhere. In addition, since by Lemma 2.1 $\text{spt}(\mu) \subset I_\delta$ for $\delta > 0$ small enough, hence $\text{spt}(\mu) \subset I_{1/4}$, we conclude that $\text{spt}(\mu)$ is concentrated on the same finite collection of $(d-1)$ -spheres centered at 0.

Step #3: we identify a lower bound for the limit contribution of the Willmore term.

Since $u(x) = 0$ a.e., we get that for almost every η ,

$$\lim_{x \rightarrow \bar{r} \pm \eta} \left[\varepsilon |\nabla u_\varepsilon(x)|^2 + \frac{1}{\varepsilon} F(u_\varepsilon(x)) \right] = \lim_{x \rightarrow \bar{r} \pm \eta} \left[\varepsilon |\nabla u_\varepsilon(x)|^2 - \frac{1}{\varepsilon} F(u_\varepsilon(x)) \right] = 0.$$

This implies in particular that

$$\frac{1}{\varepsilon} \int_{\alpha_\varepsilon}^{\beta_\varepsilon} \left(\frac{1}{2} (v'_\varepsilon)^2 - F(v_\varepsilon) \right)' dy = \int_{\bar{r}-\eta}^{\bar{r}+\eta} \left(\frac{\varepsilon}{2} (\bar{u}'_\varepsilon)^2 - \frac{1}{\varepsilon} F(\bar{u}_\varepsilon) \right)' dr \rightarrow 0.$$

By remarking that

$$\left(\frac{1}{2}(v'_\varepsilon)^2 - F(v_\varepsilon)\right)' = \mathbf{e}_\varepsilon v'_\varepsilon,$$

we can then deduce that

$$\lim_{\varepsilon \rightarrow 0} \frac{1}{\varepsilon} \int_{\alpha_\varepsilon}^{\beta_\varepsilon} \mathbf{e}_\varepsilon v'_\varepsilon dy = 0.$$

Remark 2.6. We proved previously that $\lim_{\varepsilon \rightarrow 0} \int_{\alpha_\varepsilon}^{\beta_\varepsilon} |\mathbf{e}_\varepsilon v'_\varepsilon| dy = 0$, but it does not seem to be true that $\lim_{\varepsilon \rightarrow 0} \int_{\alpha_\varepsilon}^{\beta_\varepsilon} \frac{1}{\varepsilon} |\mathbf{e}_\varepsilon v'_\varepsilon| dy = 0$.

Then, using $|1 + \varepsilon y/r_\varepsilon| \geq 1 - \eta_\varepsilon$ with $\eta_\varepsilon = 1 - \frac{\bar{r}}{r_\varepsilon} + \frac{\eta}{r_\varepsilon} \rightarrow \frac{\eta}{\bar{r}}$, it follows that

$$\begin{aligned} \frac{\sigma_\varepsilon}{\varepsilon} \int_{T_{\eta, \bar{r}}} \mathbf{eul}_\varepsilon(u_\varepsilon)^2 dx &= |S^{d-1}| r_\varepsilon^{d-1} \sigma_\varepsilon \int_{\alpha_\varepsilon}^{y_\varepsilon} \left[(-v''_\varepsilon + F'(v_\varepsilon))/\varepsilon + \frac{(d-1)/r_\varepsilon v'_\varepsilon}{1 + \varepsilon y/r_\varepsilon} \right]^2 |1 + \varepsilon y/r_\varepsilon|^{d-1} dy, \\ &\geq (1 - \eta_\varepsilon)^{d-2} |S^{d-1}| r_\varepsilon^{d-1} \sigma_\varepsilon \int_{\alpha_\varepsilon}^{y_\varepsilon} \left[(-v''_\varepsilon + F'(v_\varepsilon))/\varepsilon + \frac{(d-1)/r_\varepsilon v'_\varepsilon}{1 + \varepsilon y/r_\varepsilon} \right]^2 |1 + \varepsilon y/r_\varepsilon| dy. \end{aligned}$$

Thanks to the inequality,

$$\left[(-v''_\varepsilon + F'(v_\varepsilon))/\varepsilon + \frac{(d-1)/r_\varepsilon v'_\varepsilon}{1 + \varepsilon y/r_\varepsilon} \right]^2 \geq \frac{(d-1)^2/r_\varepsilon^2}{(1 + \varepsilon y/r_\varepsilon)^2} (v'_\varepsilon)^2 + 2 \frac{(d-1)}{r_\varepsilon(1 + \varepsilon y/r_\varepsilon)} \frac{\mathbf{e}_\varepsilon v'_\varepsilon}{\varepsilon},$$

we deduce that

$$(2.4) \quad \frac{\sigma_\varepsilon}{\varepsilon} \int_{T_{\eta, \bar{r}}} \mathbf{eul}_\varepsilon(u)^2 dx \geq A_\varepsilon + B_\varepsilon,$$

where

$$\begin{aligned} A_\varepsilon &= (1 - \eta_\varepsilon)^{d-2} |S^{d-1}| r_\varepsilon^{d-1} \frac{(d-1)^2}{r_\varepsilon^2} \sigma_\varepsilon \int_{\alpha_\varepsilon}^{\beta_\varepsilon} (1 + \varepsilon y/r_\varepsilon) (v'_\varepsilon)^2 dy \\ &\geq (1 - \eta_\varepsilon)^{d-1} |S^{d-1}| r_\varepsilon^{d-1} \frac{(d-1)^2}{r_\varepsilon^2} \sigma_\varepsilon \int_{\alpha_\varepsilon}^{\beta_\varepsilon} (v'_\varepsilon)^2 dy \end{aligned}$$

and

$$B_\varepsilon = (1 - \eta_\varepsilon)^{d-2} 2(d-1) r_\varepsilon^{d-2} |S^{d-1}| \sigma_\varepsilon \int_{\alpha_\varepsilon}^{\beta_\varepsilon} \frac{\mathbf{e}_\varepsilon v'_\varepsilon}{\varepsilon} dy \rightarrow 0.$$

For $M > 0$ and ε small enough,

$$\int_{\alpha_\varepsilon}^{\beta_\varepsilon} (v'_\varepsilon)^2 dy \geq \int_{-M}^M \left(\frac{(v'_\varepsilon)^2}{2} + F(v_\varepsilon) \right) dy + \int_{-M}^M \left(\frac{(v'_\varepsilon)^2}{2} - F(v_\varepsilon) \right) dy$$

The locally uniform convergence of $|v'_\varepsilon| - \sqrt{2F(v_\varepsilon)}$ to 0 guarantees that the second term converges to 0 as $\varepsilon \rightarrow 0^+$. As for the first term, we observe that

$$\liminf_{\varepsilon \rightarrow 0} \int_{-M}^M \left(\frac{(v'_\varepsilon)^2}{2} + F(v_\varepsilon) \right) dy \geq c_F - c_M$$

with $c_M \rightarrow 0$ as $M \rightarrow +\infty$. We deduce that

$$\liminf_{\varepsilon \rightarrow 0} A_\varepsilon \geq (1 - \frac{\eta}{\bar{r}})^{d-1} |S^{d-1}| \sigma_0 \frac{(d-1)^2}{\bar{r}^{3-d}} c_F.$$

Finally, using (2.4), the estimates above and taking the limit $\eta \rightarrow 0$, we deduce that

$$\lim_{\varepsilon \rightarrow 0} \int_{T_{\eta, \bar{r}}} \mathbf{m}_\varepsilon(u_\varepsilon) + \frac{\sigma_\varepsilon}{\varepsilon} \mathbf{eul}_\varepsilon(u_\varepsilon) dx \geq c_F |S^{d-1}| \left(\bar{r}^{d-1} + \sigma_0 \frac{(d-1)^2}{\bar{r}^{3-d}} \right).$$

Summing over all spheres, we conclude that

$$\xi \geq c_F \sum_{i \in I} \left(1 + \sigma_0 \left(\frac{d-1}{r_i} \right)^2 \right) \mathcal{H}^{d-1} \llcorner \partial B_{r_i}.$$

□

Remark 2.7. Consider a bounded subset $E \subset Q$ with C^2 boundary. Following the same arguments as in [9], one may construct a sequence $(u_\varepsilon)_\varepsilon$ such that $I_{1/4} = \partial E$ and

$$\limsup_{\varepsilon \rightarrow 0} \mathcal{E}_\varepsilon(u_\varepsilon) \leq c_F (\mathcal{P}(E) + \sigma_0 \mathcal{W}(E)).$$

A suitable sequence is for instance

$$u_\varepsilon(x) = \gamma_\varepsilon \left(\frac{\text{dist}(x, E)}{\varepsilon} \right),$$

where γ_ε is the $C^{1,1}$ truncated profile defined by

$$\gamma_\varepsilon(s) = \begin{cases} -q'(s) & \text{if } |s| \leq x_\varepsilon \\ p_\varepsilon(s) & \text{if } x_\varepsilon < |s| \leq 2x_\varepsilon \\ 0 & \text{if } |s| > 2x_\varepsilon \end{cases}$$

where $x_\varepsilon = |\log(\varepsilon)|$ and p_ε is a degree 3 polynomial satisfying

$$p_\varepsilon(x_\varepsilon) = -q'(x_\varepsilon), \quad p'_\varepsilon(x_\varepsilon) = -q''(x_\varepsilon), \quad p_\varepsilon(2x_\varepsilon) = -q'(2x_\varepsilon) \quad \text{and} \quad p'_\varepsilon(2x_\varepsilon) = 0.$$

Remark 2.8. The construction of the above remark, which is valid in arbitrary dimension, shows that both inequalities $\mu \geq c_F \sum_i \delta_{x_i}$ in Theorem 2.2 and $\xi \geq c_F \sum_{i \in I} \left(1 + \sigma_0 \frac{(d-1)^2}{r_i^2} \right) \mathcal{H}^{d-1} \llcorner \partial B_{r_i}$ in Theorem 2.5 are optimal.

Remark 2.9. The results of Theorems 2.2 and 2.5 and the above remark imply a Γ -convergence result. Consider the functional F_ε defined on the class of Radon measures in the following way: if μ_ε is a Radon measure such that there exists a radially symmetric function $u_\varepsilon \in W^{2,2}(B_R)$ satisfying $\mu_\varepsilon = \mathbf{m}_\varepsilon(u_\varepsilon) \mathcal{L}^d$ then $F_\varepsilon(\mu_\varepsilon) = \mathcal{E}_\varepsilon(u_\varepsilon, B_R)$, otherwise $F_\varepsilon(\mu_\varepsilon) = +\infty$. Let F be the functional defined for Radon measures on Q in the following way: if μ is a Radon measure such that

$$\mu = c_F \sum_{i \in I} m_i \mathcal{H}^{d-1} \llcorner \partial B_{r_i}$$

where the collection $\{(r_i, m_i), i \in I\}$ is finite, all r_i 's are positive real numbers with $r_i < R$ and all m_i 's are positive integers, then

$$F(\mu) = c_F |S^{d-1}| \sum_{i \in I} m_i \left(r_i^{d-1} + \sigma_0 \frac{(d-1)^2}{r_i^{3-d}} \right)$$

and $F(\mu) = +\infty$ otherwise. It follows from the above results that the Γ -limit of F_ε is well defined for all Radon measures μ of the form

$$\mu = c_F \sum_{i \in I} \mathcal{H}^{d-1} \llcorner \partial B_{r_i}, \quad I \text{ finite, } 0 < r_i < R$$

and coincides with F on such measures, i.e.,

$$(\Gamma - \lim F_\varepsilon)(c_F \sum_{\substack{i \in I \\ I \text{ finite} \\ 0 < r_i < R}} \mathcal{H}^{d-1} \llcorner \partial B_{r_i}) = c_F |S^{d-1}| \sum_{i \in I} m_i \left(r_i^{d-1} + \sigma_0 \frac{(d-1)^2}{r_i^{3-d}} \right).$$

The Γ -convergence in general should be true as well but requires to check that the limit measure has necessarily the form $c_F \sum_{i \in I} m_i \mathcal{H}^{d-1} \llcorner \partial B_{r_i}$.

3. NUMERICAL EXPERIMENTS

We propose in this section a simple numerical scheme to approximate the L^2 -gradient flow of \mathcal{E}_ε , whose definition for $u \in W^{2,2}(Q)$ satisfying $0 \leq u \leq 1/4$ is recalled:

$$\mathcal{E}_\varepsilon(u, Q) = \int_Q \left(\frac{\varepsilon}{2} |\nabla u|^2 + \frac{1}{\varepsilon} F(u) \right) dx + \frac{\sigma_\varepsilon}{2\varepsilon} \int_Q \left(\varepsilon \Delta u - \frac{1}{\varepsilon} F'(u) \right)^2 dx,$$

Its L^2 -gradient flow is described, up to a time rescaling, by the system

$$(3.1) \quad \begin{cases} u_t &= \mu + \sigma_\varepsilon \left(-\Delta \mu + \frac{1}{\varepsilon^2} F''(u) \mu \right) \\ \mu &= \Delta u - \frac{1}{\varepsilon^2} F'(u). \end{cases}$$

The numerical approximation of the solutions will be performed in a square calculation box Q with periodic boundary conditions.

Our primary objective in this section is to demonstrate that the numerical solutions to the phase field flow starting from the initial condition $u(x, 0) = -q'(\text{dist}(\Gamma, x)/\varepsilon)$ are accurate approximations, at least in the regular case, of the non-oriented mean curvature flow $t \mapsto \Gamma(t)$ starting from $\Gamma(0) = \Gamma$. Here, dist denotes the classical distance function.

Given a positive time discretization parameter δ_t , we now review several classical schemes used to construct sequences $(u^n)_{n \geq 0}$ that approximate exact solutions $u(\cdot, n\delta_t)$ of (3.1).

Due to the homogeneity of the differential operators involved, a fast semi-implicit Fourier spectral method as in [26, 17, 20, 23, 21, 19] can be employed, see also [34] for a recent review of numerical methods for phase fields approximations of various geometric flows.

Recall that the Fourier \mathbf{K} -approximation of a function u defined in Q is given by

$$u^{\mathbf{K}}(x) = \sum_{\mathbf{k} \in K_N} c_{\mathbf{k}} e^{2i\pi \xi_{\mathbf{k}} \cdot x},$$

where $K_N = [-\frac{N_1}{2}, \frac{N_1}{2} - 1] \times [-\frac{N_2}{2}, \frac{N_2}{2} - 1] \cdots \times [-\frac{N_d}{2}, \frac{N_d}{2} - 1]$, $\mathbf{k} = (k_1, \dots, k_d)$ and $\xi_{\mathbf{k}} = (k_1/\ell_1, \dots, k_d/\ell_d)$. In this expression, the coefficients $c_{\mathbf{k}}$'s denote the first discrete Fourier coefficients of u . The inverse discrete Fourier transform (IFFT) gives the values of $u^{\mathbf{K}}$ at points $x_{\mathbf{k}} = (k_1 h_1, \dots, k_d h_d)$, $h_\alpha = \ell_\alpha / N_\alpha$ for $\alpha \in \{1, \dots, d\}$, more precisely $u_{\mathbf{k}}^{\mathbf{K}} = \text{IFFT}[c_{\mathbf{k}}]$. Conversely, $c_{\mathbf{k}}$ can be computed as the discrete Fourier transform of $u_{\mathbf{k}}^{\mathbf{K}}$, i.e. $c_{\mathbf{k}} = \text{FFT}[u_{\mathbf{k}}^{\mathbf{K}}]$.

Semi-implicit approaches typically treat explicitly the nonlinear terms of phase field models, which requires stabilization techniques to ensure computational efficiency.

In this context, a well-known approach proposed by Eyre in [37] uses a convex-concave splitting of the Cahn-Hilliard energy. This method provides a simple, effective, and stable scheme for approximating various evolution problems with gradient flow structures, as illustrated in [30, 60, 39, 36, 55, 56, 52]. More recent approaches stabilize these schemes by introducing relaxation techniques based on the *Scalar Auxiliary Variable* (SAV) method. These methods have

been used in a wide variety of studies [40, 53, 54, 1, 41] to address a broad class of gradient flow systems, particularly the Cahn-Hilliard equation [58, 42, 61, 18], dissipative systems [16, 62], and their variants [44, 43].

In the remainder of this paper, we will focus exclusively on the convex-concave splitting approach, which is simpler to implement.

The code used for the numerical experiments described in the next paragraphs is available on a GitHub¹ repository.

3.1. A convex-concave Fourier spectral numerical method. Consider the gradient flow of an energy \mathcal{E}_ε

$$\varepsilon \partial_t u = -\nabla_u \mathcal{E}_\varepsilon(u),$$

and decompose \mathcal{E}_ε as the sum of a convex energy $\mathcal{E}_{\varepsilon,c}$ and a concave energy $\mathcal{E}_{\varepsilon,e}$ (a classical explicit decomposition will be proposed later):

$$\mathcal{E}_\varepsilon = \mathcal{E}_{\varepsilon,c} + \mathcal{E}_{\varepsilon,e}.$$

An effective numerical scheme associated with this decomposition can be designed by integrating implicitly the gradient of the convex part, and explicitly the gradient of the concave part:

$$\varepsilon \frac{u^{n+1} - u^n}{\delta_t} = -(\nabla_u \mathcal{E}_{\varepsilon,c}(u^{n+1}) + \nabla_u \mathcal{E}_{\varepsilon,e}(u^n)).$$

The energy stability can be easily proven by interpreting this scheme as one step, starting from u^n , of the implicit discretization of the semi-linearized PDE $\partial_t u = -\nabla_u \bar{\mathcal{E}}_{\varepsilon,u^n}(u)$ where $\bar{\mathcal{E}}_{\varepsilon,u^n}$ is defined as

$$\bar{\mathcal{E}}_{\varepsilon,u^n}(u) = \mathcal{E}_{\varepsilon,c}(u) + \mathcal{E}_{\varepsilon,e}(u^n) + \langle \nabla_u \mathcal{E}_{\varepsilon,e}(u^n), (u - u^n) \rangle.$$

It is easily seen that $\bar{\mathcal{E}}_{\varepsilon,u^n}(u^{n+1}) \leq \bar{\mathcal{E}}_{\varepsilon,u^n}(u^n)$. Using the concavity of $\mathcal{E}_{\varepsilon,e}$ it can be proved that the energy \mathcal{E}_ε decreases along the iterations:

$$\mathcal{E}_\varepsilon(u^{n+1}) \leq \mathcal{E}_\varepsilon(u^n).$$

For our phase field model

$$\mathcal{E}_\varepsilon(u, Q) = \int_Q \left(\frac{\varepsilon}{2} |\nabla u|^2 + \frac{1}{\varepsilon} F(u) \right) dx + \frac{\sigma_\varepsilon}{2\varepsilon} \int_Q \left(\varepsilon \Delta u - \frac{1}{\varepsilon} F'(u) \right)^2 dx,$$

we define, using $\alpha, \beta > 0$, the convex energy

$$\mathcal{E}_{\varepsilon,c}(u, Q) = \frac{\varepsilon}{2} \int_Q (|\nabla u|^2 + \sigma_\varepsilon (\Delta u)^2 + \alpha u^2 + \beta |\nabla u|^2) dx.$$

For sufficiently large coefficients α, β , the energy

$$\mathcal{E}_{\varepsilon,e}(u, Q) = \frac{\varepsilon}{2} \int_Q \left(\frac{2}{\varepsilon^2} F(u) + \sigma_\varepsilon \left((\Delta u - \frac{1}{\varepsilon^2} F'(u))^2 - (\Delta u)^2 \right) - \alpha u^2 - \beta |\nabla u|^2 \right) dx,$$

is concave, at least on a subset of $W^{2,2}(Q)$ where the energy $\mathcal{E}_\varepsilon(\cdot, Q)$ is bounded. The numerical scheme associated with the decomposition $\mathcal{E}_\varepsilon = \mathcal{E}_{\varepsilon,c} + \mathcal{E}_{\varepsilon,e}$ is given by

$$u^{n+1} = L[g(u^n)],$$

¹<https://github.com/eliebretin/UMCF.git>

where g is a nonlinear operator defined by

$$g(u) = u + dt \left(-\frac{F'(u)}{\varepsilon^2} + \sigma_\varepsilon \left(-\Delta[F'(u)/\varepsilon^2] + \frac{F''(u)}{\varepsilon^2} [\Delta u - F'(u)/\varepsilon^2] \right) + \alpha u - \beta \Delta u \right),$$

and L is the homogeneous linear operator $(I_d + \delta_t(-\Delta + \sigma_\varepsilon \Delta^2 + \alpha I_d - \beta \Delta))^{-1}$, whose Fourier symbol is

$$\hat{L}(\xi) = 1/(1 + \delta_t(4\pi^2|\xi|^2 + \sigma_\varepsilon 16\pi^4|\xi|^4 + \alpha + \beta 4\pi^2|\xi|^2)).$$

Remark 3.1. In the scheme above, we have not taken into account the singularity of F for values greater than $1/4$. A straightforward way to address this issue and incorporate it into our scheme is by introducing a projection step:

$$u^{n+1} = \min(L[g(u^n)], 1/4).$$

Remark 3.2. Using the parameters α, β in the convex-concave splitting ensures high stability of the numerical scheme. However, it generally results in reduced accuracy. As the main purpose of the numerical results presented in the next sections is to compare precisely our flow with the mean curvature flow, we need high accuracy. So we opt for the settings $\alpha = \beta = 0$ to avoid accuracy losses and a time step $\delta_t = 0.01\varepsilon^2$ significantly below the natural stability condition of the PDE. Readers who are not so demanding in terms of precision, but who are interested in stable simulations obtained with larger time steps might opt for positive values of α, β , typically $\alpha = \frac{1}{\varepsilon^2}, \beta = 1$, and a time step $\delta_t = \varepsilon^2$.

3.2. 2D numerical simulations. We first focus on evolving interfaces confined in $Q = [0, 1]^2$ discretized with N nodes in both directions.

3.2.1. Evolution of a circle and comparison with mean curvature flow. A circle of initial radius R_0 flowing by mean curvature remains a circle with radius given by

$$R(t) = \sqrt{R_0^2 - 2t}$$

until the extinction time $t_{end} = \frac{1}{2}R_0^2$. In our first numerical experiment, we compare this evolution with the flow provided by our phase field model for two different values of ε .

We set $N = 2^8$, $\varepsilon = 1.5/N$ or $\varepsilon = 3/N$, $\sigma_\varepsilon = 4\varepsilon^2$, $\alpha = \beta = 0$ and $\delta_t = 0.01\varepsilon^2$. This time step setting, well below the natural stability condition, is more suitable to illustrate numerically the convergence order of the phase field model with respect to ε , while drastically reducing the numerical discretization errors.

Figure 4 shows several iterates u^n for the setting $\varepsilon = 1.5/N$ and $\varepsilon = 3/N$. The influence of the parameter ε on the size of the diffuse interface is clearly observable. Furthermore, the initial circle appears to evolve in a consistent manner, with its radius decreasing over the iterations. To compare the radius law with the theoretical law of motion by mean curvature, we plot in Figure 5 a comparison between the different evolutions $t \mapsto R(t)$. Specifically, the approximate radius $R_\varepsilon(t)$ is estimated from the phase field function $u_\varepsilon(t)$ using the formula

$$R_\varepsilon = \frac{1}{2\pi\varepsilon} \int_Q u_\varepsilon dx.$$

Notably, the left side of Figure 5 shows that the two laws obtained with $\varepsilon = 1.5/N$ and $\varepsilon = 3/N$ are very close to the theoretical one. A zoom on the interval $[0.058, 0.068]$ shown on the right side of Figure 5 indicates that the observed error is approximately twice as significant

when using $\varepsilon = 3/N$ compared to $\varepsilon = 1.5/N$. This suggests that our phase field model should converge to the mean curvature flow with an error of order $O(\varepsilon)$. In contrast, this error is typically of order $O(\varepsilon^2)$ for the Allen-Cahn equation.

This numerical result goes well beyond our initial theoretical expectations: we expected the phase field profile to be stable for sufficiently large choices of σ_ε , but we did not expect the approximate flow to approximate well the mean curvature flow. To theoretically justify such a result, we would need to adapt the asymptotic developments of Allen-Cahn solutions to the context of non-oriented phase field functions.

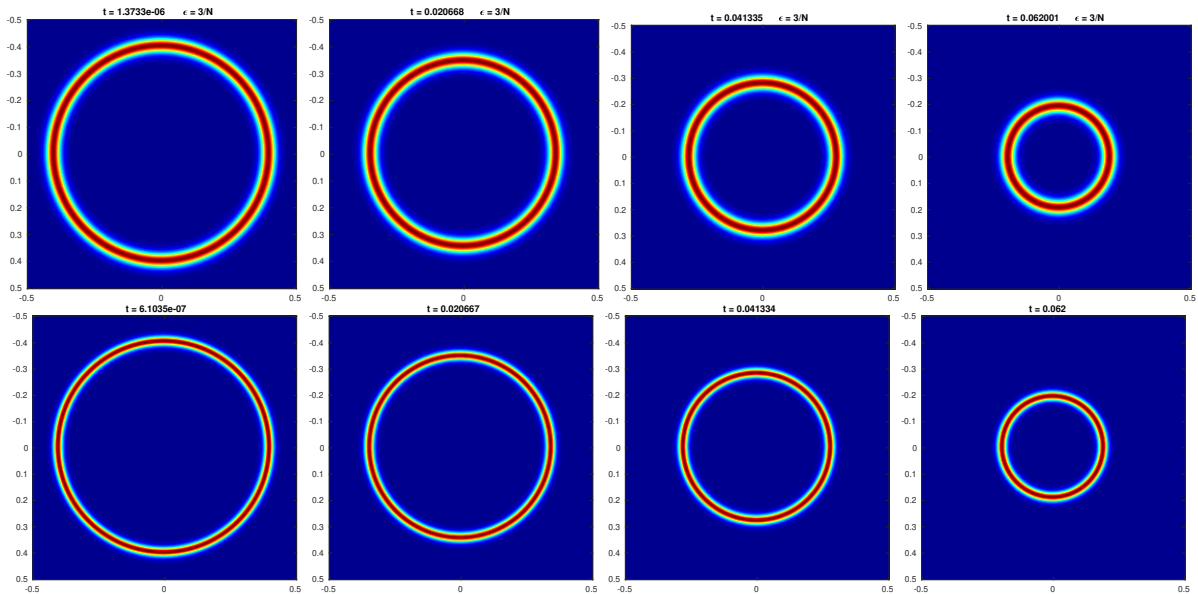


FIGURE 4. Approximate evolution of a circle across iterations using two values of ε : first line with $\varepsilon = 3/N$, second line with $\varepsilon = 1.5/N$.

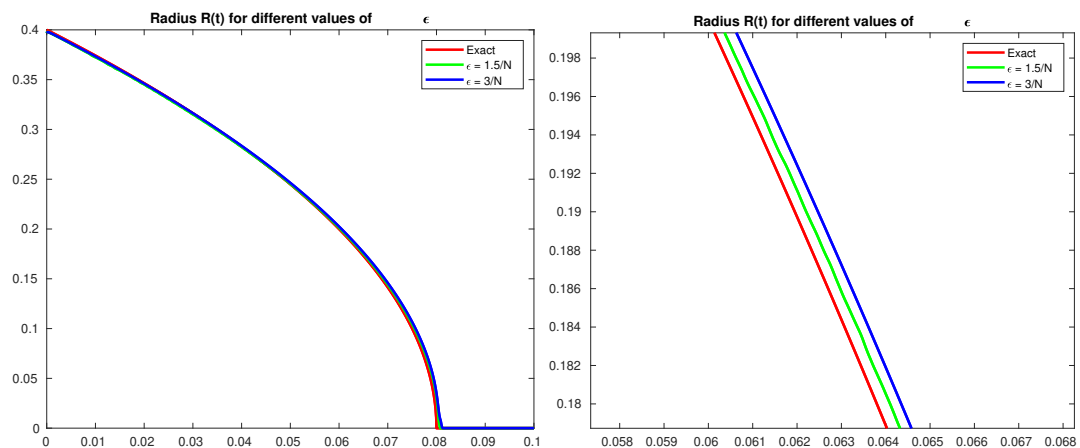


FIGURE 5. Comparison of the numerical radius of the circle evolved with our model vs the exact radius $t \mapsto R(t)$ provided by mean curvature flow. Left: on the time interval $[0, 0.1]$. Right: zoom on the time interval $[0.058, 0.068]$.

3.2.2. *Influence on stability of parameter σ_ε .* The second numerical experiment aims to demonstrate the influence of parameter σ_ε on the stability of interfaces evolving by our phase field flow. We have already justified in the analysis of the model the importance of σ_ε as ε approaches 0. Here, we aim to illustrate numerically that the choice of this parameter is not trivial and must be made with care. Specifically, a parameter that is too small may fail to ensure the stability of the interface, while a parameter that is excessively large can increase the computational cost and amplify the contribution of the Willmore term in the flow.

Figure 6 illustrates three different evolutions $t \rightarrow u_\varepsilon(t)$ obtained using $\sigma_\varepsilon = \varepsilon^2$, $\sigma_\varepsilon = 2\varepsilon^2$ and $\sigma_\varepsilon = 4\varepsilon^2$. The other parameters remain constant: $N = 2^8$, $\varepsilon = 2/N$, $\delta_t = 0.01\varepsilon^2$ and $\alpha = \beta = 0$.

We first observe that the choice $\sigma_\varepsilon = \varepsilon^2$ does not ensure the stability of the interface. Surprisingly, the interfaces with low curvature appear to be the most unstable.

The second row of Figure 6, corresponding to $\sigma_\varepsilon = 2\varepsilon^2$, shows an evolution that looks better. However, upon examining the second figure more closely, we note that the profile does not fully reach the value of $1/4$ when the curvature is zero, indicating that the evolution is not completely stable. In contrast, the choice $\sigma_\varepsilon = 4\varepsilon^2$ seems to ensure, at least in this example, a satisfactory diffuse profile across the entire interface long the iterations.

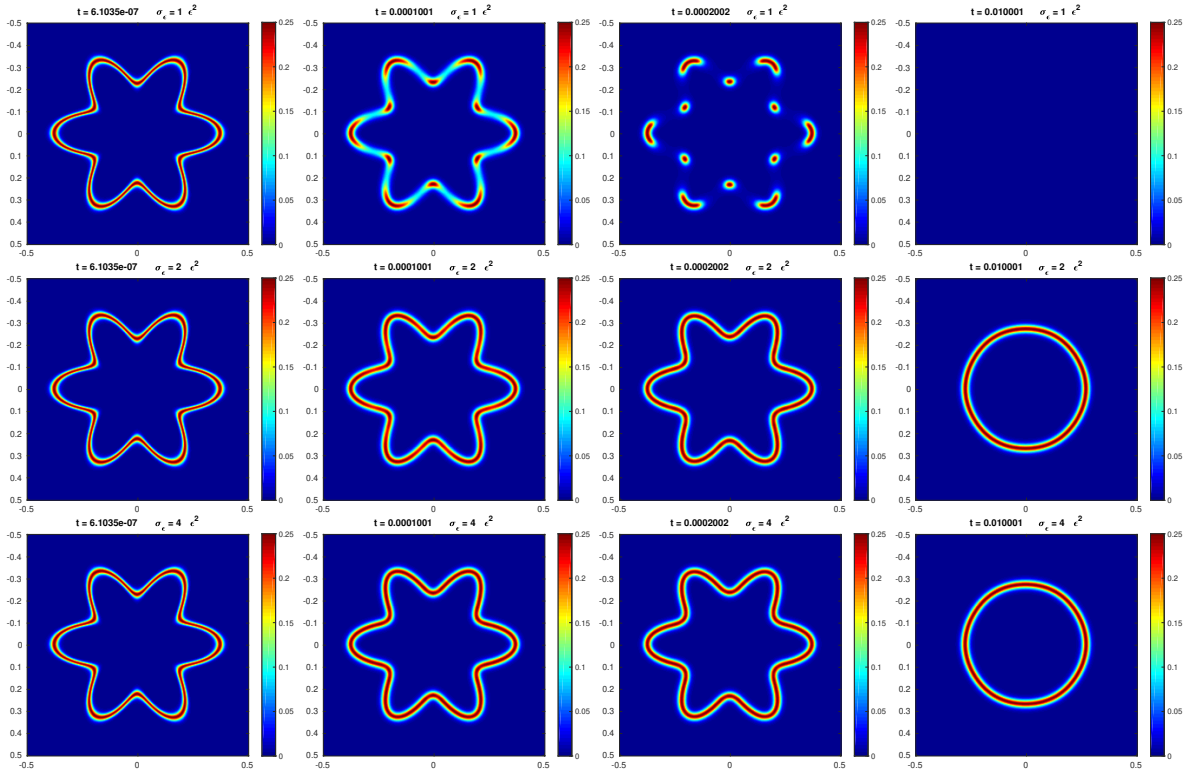


FIGURE 6. Evolution of a shape for three values of σ_ε . First line: $\sigma_\varepsilon = \varepsilon^2$, second line: $\sigma_\varepsilon = 2\varepsilon^2$, third line: $\sigma_\varepsilon = 4\varepsilon^2$.

3.2.3. *Non smooth interfaces and evolution of triple junctions.* The aim of this next numerical experiment is to demonstrate that the proposed phase field model can effectively handle the evolution of singular interfaces with triple junctions. We consider two examples where the initial condition involves either two or three glued circles. The mean curvature flow of these shapes

cannot be approximated with the classical Allen-Cahn equation, it is necessary to use a multiphase Allen-Cahn model where the interior of each circle represents a distinct phase. Across iterations produced by this multiphase model, the angles between phases at triple points evolve toward Herring’s equiangular equilibrium configuration. The numerical simulations obtained with our approach are presented in Figure 7, revealing stable triple points that exhibit a quasi-symmetry consistent with Herring’s law. The numerical results closely resemble the outcomes that a multiphase model would yield. For this experiment, we set $N = 2^8$, $\varepsilon = 2/N$, $\sigma_\varepsilon = 4\varepsilon^2$, $\delta_t = 0.1\varepsilon^2$ and $\alpha = \beta = 0$.

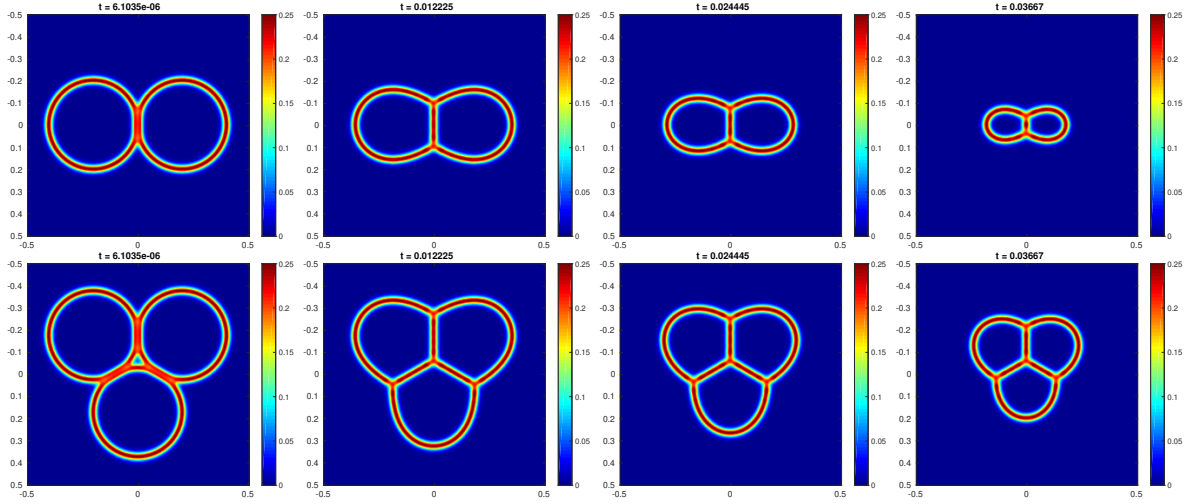


FIGURE 7. Non-smooth evolving shapes. Each row corresponds to a different initial condition. The figures show the phase field across iterations.

3.3. 3D numerical simulations. As in the two-dimensional case, we first examine the evolution of a sphere. The other experiments illustrate the influence of the Willmore term in our model. It not only ensures the stability of the interface, it also plays a significant role when the interface undergoes topological changes, as in the case of a dumbbell flowing by mean curvature. An interesting aspect of the Willmore term is its ability to stabilize fine structures, such as tubular sets, which is not achievable with conventional mean curvature approximation models. We will illustrate this point by showing how our phase field model can approximate well the mean curvature flow of thin structures of codimension two, such as circles or, more generally, tubular sets.

In all subsequent numerical experiments, we display the $\frac{1}{6}$ -level set of each approximate solution u_ε to represent the evolving interface associated to the phase field function u_ε (recall that the potential F satisfies $F'(\frac{1}{6}) = 0$).

3.3.1. Evolution of a sphere and comparison with mean curvature flow. An initial sphere of radius R_0 flowing by mean curvature remains a sphere whose radius satisfies the law $R(t) = \sqrt{R_0 - 4t}$. In the first three images of Figure 8, we display the $\frac{1}{6}$ -level set of the phase field function u_ε provided by our numerical model at three different iterations. The computation was made using the numerical parameters $N = 2^7$, $\varepsilon = 2/N$, $\sigma_\varepsilon = 2\varepsilon^2$, $\delta_t = 0.01\varepsilon^2$ and $\alpha = \beta = 0$. The evolving shape closely resembles a sphere with radius decreasing over time. The last image of Figure 8 plots the numerical radius of the shapes computed across iterations

using the formula $R_\varepsilon = \sqrt{\frac{1}{4\pi\varepsilon} \int u_\varepsilon dx}$. The evolution of the numerical radius closely aligns with the theoretical law, although the error appears to be larger than in the two-dimensional case. This could be due the parameter settings, in particular the resolution is coarser than the resolution used in 2D.

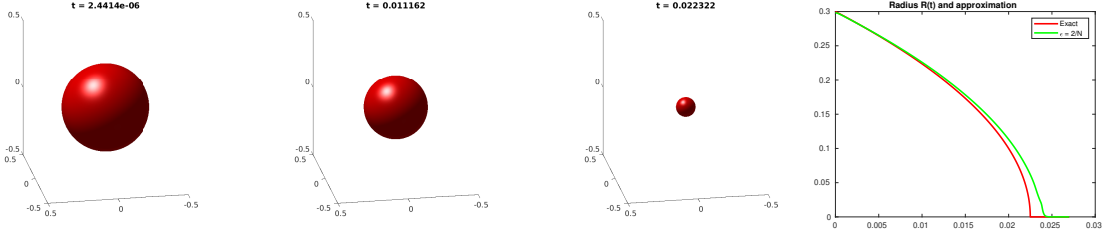


FIGURE 8. Evolution obtained with our model starting from an initial sphere, and comparison of the numerical radius with the radius of a sphere evolving exactly by mean curvature.

3.3.2. *Evolution of a dumbbell and influence of the Willmore term.* A classical example of mean curvature flow where singularities appear in finite time is the evolution of a dumbbell. The classical Allen-Cahn model provides an approximate mean curvature flow beyond singularities which is compatible with Brakke’s notion of weak mean curvature flow. When singularities appear, the dumbbell moved by the Allen-Cahn model separates into two sphere-type shapes that evolve until they vanish. In the proposed numerical experiment, we apply our model to a dumbbell, noting that the Willmore term is expected to prevent singular interfaces, thus topological changes. This is indeed what we observe in the two numerical experiments shown in Figure 9, where each row corresponds to different values of ε . The experiments were carried out with the following parameters: $N = 2^7$, $\varepsilon = 2/N$, $\sigma_\varepsilon = 2\varepsilon^2$, $\delta_t = 0.01\varepsilon^2$ and $\alpha = \beta = 0$. In both cases the two sphere-type shapes remain connected by a cylinder, the thickness of the cylinder being directly related to the value of ε . Notably, the cylinder appears to have minimal influence on the dynamics, probably because its lowest principal curvature is zero.

A preliminary conclusion is that our model effectively approximates the smooth mean curvature flow before the singularities begin to appear, a point at which the Willmore term begins to have a substantial impact on the flow.

3.3.3. *Interfaces with triple junctions.* We illustrate in Figure 10 the evolution by our phase field model of two-dimensional shapes in 3D made of two or three spheres glued together. Like in the two-dimensional case, the evolution is consistent with the result that would provide a multiphase approach, exhibiting triple lines that evolve to satisfy Herring’s equilibrium conditions.

3.3.4. *Evolution of tubular sets with triple junctions.* As observed in a previous experiment, the Willmore term ensures the stability of the phase field profile, and its geometric properties guarantee the stability of thin structures. We illustrate now that our approach can effectively approximate the mean curvature flow of sets of codimension two represented approximately by tubular structures. The first example involves the evolution of a circle in dimensions three. In Figure 11, we display the level set $1/6$ across iterations of a solution u_ε approximating the evolution of a 1D circle in 3D. The parameters are $N = 2^7$, $\varepsilon = 2/N$, $\sigma_\varepsilon = 2\varepsilon^2$, $\delta_t = 0.01\varepsilon^2$ and

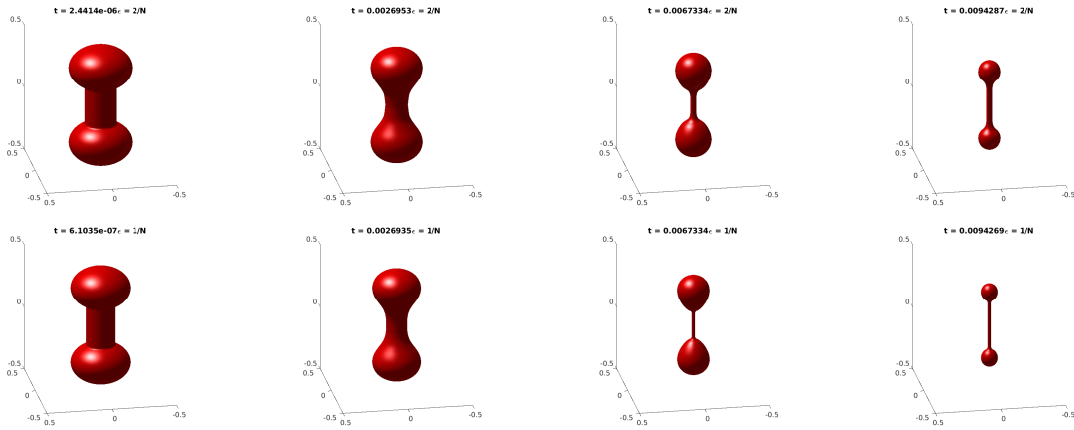


FIGURE 9. A dumbbell flowed by our phase field model, for two different values of ε .

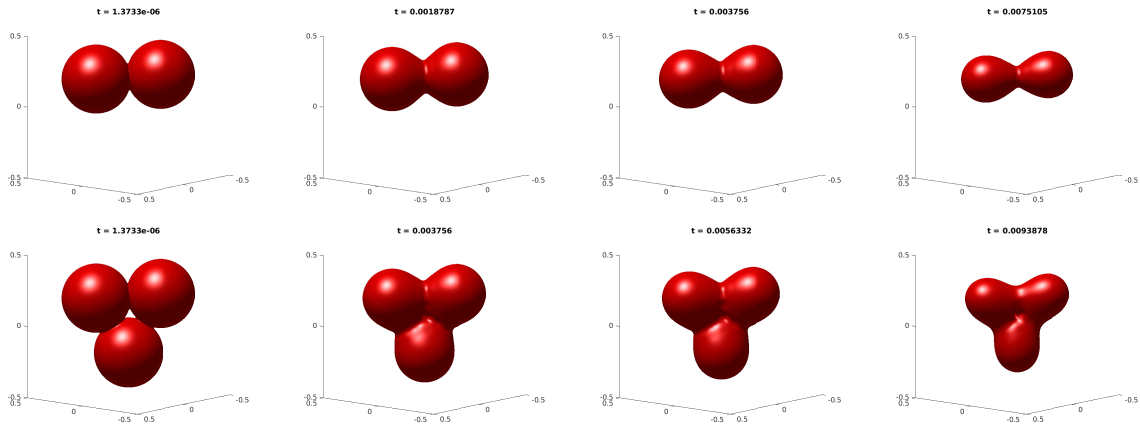


FIGURE 10. Two nonsmooth shapes evolved by our model.

$\alpha = \beta = 0$. As anticipated, the shapes approximate circles with radius decreasing over time. A closer look at the radius law reveals that it is consistent with a motion by mean curvature, differing only by a multiplicative factor.

Finally, we present in Figure 11 the last numerical experiments performed on two filaments with periodic boundary conditions, one with triple points, the other without. Both filaments evolve toward minimal sets.

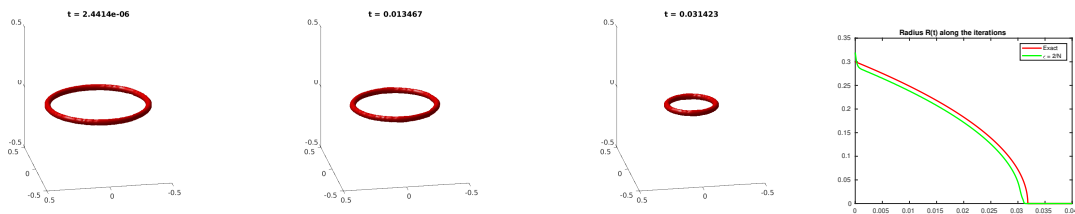


FIGURE 11. Evolution with our model of an approximate circle in 3D, and comparison of its radius with the exact radius law of mean curvature flow.

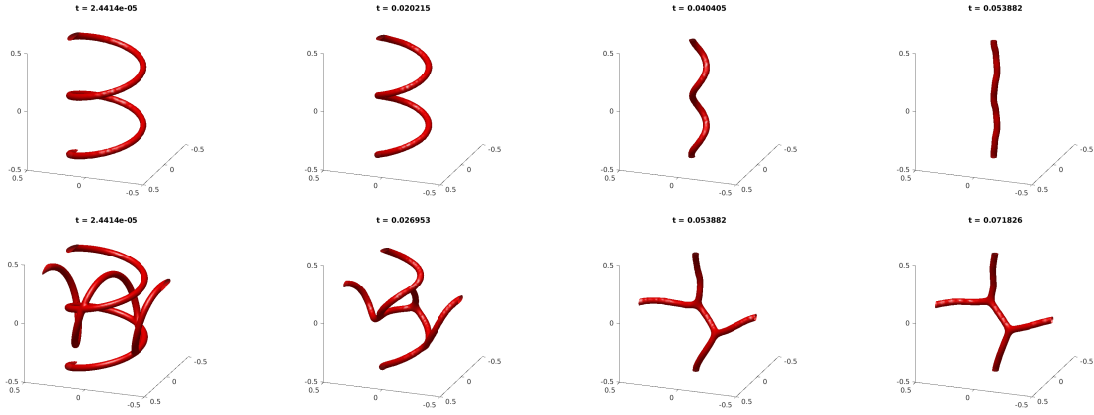


FIGURE 12. Evolution of two tubular sets with periodic boundary conditions

4. CONCLUSION AND REMARKS

In this paper, we have introduced and studied a Cahn-Hilliard-type energy coupled with a phase-field Willmore-type energy. A key aspect of our contribution is the use in the Cahn-Hilliard-type energy of a specific potential that combines a smooth well at $s = 0$ and an obstacle at $s = 1/4$. Our variational model admits a regular minimizer connecting these two phases, and the Willmore term not only promotes the stability of this regular profile along the gradient flow, it also imposes a penalty on the $s = 1/4$ phase which facilitates the approximation of the surface tension energy of non-oriented interfaces. The asymptotic analysis of our model in dimension 1, and in higher dimensions for radial functions, has enabled us to justify more rigorously these properties and the relevance of the new potential.

A surprising and theoretically unjustified result is that the L^2 gradient flow of our energy is, at least numerically, a fairly good approximation of the mean curvature flow of codimension 1 or 2 surfaces, which allows for the presence of triple junctions. A promising next step would be to justify this numerical observation by adapting classical asymptotic expansion techniques to our context. Additionally, it would be interesting to analyze the profiles of the solution at triple junctions and to identify more precisely the profile observed in the case of tubular sets, which likely does not correspond to the profile $-q'$ mentioned in the introduction.

ACKNOWLEDGEMENTS

The authors acknowledge support from the "France 2030" funding ANR-23-PEIA-0004 ("PDE-AI") and from the French National Research Agency (ANR) under grants ANR-19-CE01-0009-01 (project MIMESIS-3D) and ANR-24-CE40-XXX (project STOIQUES). Part of this work was also supported by the LABEX MILYON (ANR-10-LABX-0070) of Université de Lyon, within the program "Investissements d'Avenir" (ANR-11-IDEX-0007) operated by the French National Research Agency (ANR), and by the European Union Horizon 2020 research and innovation programme under the Marie Skłodowska-Curie grant agreement No 777826 (NoMADS).

REFERENCES

- [1] G. Akrivis, B. Li, and D. li. Energy-decaying extrapolated RK-SAV methods for the Allen-Cahn and Cahn-Hilliard equations. *SIAM Journal on Scientific Computing*, 41(6):A3703–A3727, 2019. 21

- [2] L. Ambrosio. Geometric evolution problems, distance function and viscosity solutions. In *Calculus of variations and partial differential equations (Pisa, 1996)*, pages 5–93. Springer, Berlin, 2000. [3](#)
- [3] L. Ambrosio and V. M. Tortorelli. On the approximation of free discontinuity problems. *Boll. Un. Mat. Ital. B* (7), 6(1):105–123, 1992. [2](#), [5](#)
- [4] G. Bellettini. *Lecture notes on mean curvature flow, barriers and singular perturbations*, volume 12 of *Appunti. Scuola Normale Superiore di Pisa (Nuova Serie) [Lecture Notes. Scuola Normale Superiore di Pisa (New Series)]*. Edizioni della Normale, Pisa, 2013. [3](#)
- [5] G. Bellettini, M. Freguglia, and N. Picenni. On a conjecture of De Giorgi about the phase-field approximation of the Willmore functional. *Arch. Ration. Mech. Anal.*, 247(3):Paper No. 39, 37, 2023. [4](#)
- [6] G. Bellettini and L. Mugnai. On the approximation of the elastica functional in radial symmetry. *Calc. Var. Partial Differential Equations*, 24:1–20, 2005. [4](#), [10](#)
- [7] G. Bellettini and M. Paolini. Approssimazione variazionale di funzionali con curvatura. In *Seminario Analisi Matematica, Univ. Bologna*, pages 87–97, 1993. [2](#), [4](#)
- [8] G. Bellettini and M. Paolini. Quasi-optimal error estimates for the mean curvature flow with a forcing term. *Differential Integral Equations*, 8(4):735–752, 1995. [3](#)
- [9] G. Bellettini and M. Paolini. Anisotropic motion by mean curvature in the context of Finsler geometry. *Hokkaido Math. J.*, 25:537–566, 1996. [19](#)
- [10] J. F. Blowey and C. M. Elliott. The Cahn–Hilliard gradient theory for phase separation with non-smooth free energy part ii: Numerical analysis. *European Journal of Applied Mathematics*, 3(2):147–179, 1992. [4](#)
- [11] M. Bonafini, G. Orlandi, and E. Oudet. Variational approximation of functionals defined on 1-dimensional connected sets: the planar case. *SIAM J. Math. Anal.*, 50(6):6307–6332, 2018. [6](#)
- [12] M. Bonafini and E. Oudet. A convex approach to the Gilbert–Steiner problem. *Interfaces Free Bound.*, 22(2):131–155, 2020. [6](#)
- [13] M. Bonnivard, E. Bretin, and A. Lemenant. Numerical approximation of the Steiner problem in dimension 2 and 3. *Math. Comp.*, 89(321):1–43, 2020. [6](#)
- [14] M. Bonnivard, A. Lemenant, and F. Santambrogio. Approximation of length minimization problems among compact connected sets. *SIAM J. Math. Anal.*, 47(2):1489–1529, 2015. [6](#)
- [15] G. Bouchitté, C. Dubs, and P. Seppecher. Transitions de phases avec un potentiel dégénéré à l’infini, application à l’équilibre de petites gouttes. *C. R. Acad. Sci. Paris Sér. I Math.*, 323(9):1103–1108, 1996. [2](#)
- [16] A. Bouchriti, M. Pierre, and N. E. Alaa. Remarks on the asymptotic behavior of scalar auxiliary variable (SAV) schemes for gradient-like flows. *J. Appl. Anal. Comput.*, 10(5):2198–2219, 2020. [21](#)
- [17] M. Brassel and E. Bretin. A modified phase field approximation for mean curvature flow with conservation of the volume. *Math. Methods Appl. Sci.*, 34(10):1157–1180, 2011. [20](#)
- [18] E. Bretin, L. Calatroni, and S. Masnou. A mobility-SAV approach for a Cahn–Hilliard equation with degenerate mobilities. *Discrete Contin. Dyn. Syst. Ser. S*, 17(1):131–159, 2024. [21](#)
- [19] E. Bretin, A. Danescu, J. Penuelas, and S. Masnou. Multiphase mean curvature flows with high mobility contrasts: A phase-field approach, with applications to nanowires. *Journal of Computational Physics*, 365:324–349, 2018. [20](#)
- [20] E. Bretin, F. Dayrens, and S. Masnou. Volume reconstruction from slices. *SIAM J. Imaging Sci.*, 10(4):2326–2358, 2017. [20](#)
- [21] E. Bretin, R. Denis, J.-O. Lachaud, and E. Oudet. Phase-field modelling and computing for a large number of phases. *ESAIM:M2AN*, 53(3):805–832, 2019. [20](#)
- [22] E. Bretin, R. Denis, S. Masnou, and G. Terii. Learning phase field mean curvature flows with neural networks. *J. Comput. Phys.*, 470:Paper No. 111579, 28, 2022. [1](#), [2](#), [6](#), [7](#)
- [23] E. Bretin and S. Masnou. A new phase field model for inhomogeneous minimal partitions, and applications to droplets dynamics. *Interfaces and Free Boundaries*, 19:141–182, 01 2017. [20](#)
- [24] E. Bretin, S. Masnou, and E. Oudet. Phase-field approximations of the Willmore functional and flow. *Numer. Math.*, 131(1):115–171, 2015. [2](#), [4](#), [5](#)
- [25] A. Chambolle, L. A. D. Ferrari, and B. Merlet. A phase-field approximation of the Steiner problem in dimension two. *Adv. Calc. Var.*, 12(2):157–179, 2019. [6](#)
- [26] L. Chen and J. Shen. Applications of semi-implicit Fourier-spectral method to phase field equations. *Computer Physics Communications*, 108:147–158, 1998. [20](#)

- [27] X. Chen. Generation and propagation of interfaces for reaction-diffusion equations. *J. Differential Equations*, 96(1):116–141, 1992. [3](#)
- [28] X. Chen. Global asymptotic limit of solutions of the Cahn-Hilliard equation. *J. Differential Geom.*, 44(2):262–311, 1996. [10](#)
- [29] X. Chen and C. M. Elliott. Asymptotics for a parabolic double obstacle problem. *Proc. Roy. Soc. London Ser. A*, 444(1922):429–445, 1994. [4](#)
- [30] M. Cheng and J. A. Warren. An efficient algorithm for solving the phase field crystal model. *J. Comput. Phys.*, 227(12):6241–6248, 2008. [20](#)
- [31] G. David. *Singular sets of minimizers for the Mumford-Shah functional*, volume 233 of *Progress in Mathematics*. Birkhäuser Verlag, Basel, 2005. [5](#)
- [32] E. De Giorgi. Some remarks on Γ -convergence and least square methods. In G. D. Maso and G. Dell’Antonio, editors, *Composite Media and Homogenization Theory*, pages 135–142. Birkhäuser, Boston, 1991. [4](#)
- [33] P. de Mottoni and M. Schatzman. Geometrical evolution of developed interfaces. *Trans. Amer. Math. Soc.*, 347(5):1533–1589, 1995. [3](#)
- [34] Q. Du and X. Feng. Chapter 5 - The phase field method for geometric moving interfaces and their numerical approximations. In A. Bonito and R. H. Nochetto, editors, *Geometric Partial Differential Equations - Part I*, volume 21 of *Handbook of Numerical Analysis*, page 425–508. Elsevier, 2020. [20](#)
- [35] C. M. Elliott and R. Schätzle. The limit of the anisotropic double-obstacle Allen–Cahn equation. *Proceedings of the Royal Society of Edinburgh: Section A Mathematics*, 126(6):1217–1234, 1996. [4](#)
- [36] M. Elsey and B. Wirth. A simple and efficient scheme for phase field crystal simulation. *ESAIM Math. Model. Numer. Anal.*, 47(5):1413–1432, 2013. [20](#)
- [37] D. J. Eyre. Unconditionally gradient stable time marching the Cahn-Hilliard equation. In *Computational and mathematical models of microstructural evolution (San Francisco, CA, 1998)*, volume 529 of *Mater. Res. Soc. Sympos. Proc.*, pages 39–46. MRS, Warrendale, PA, 1998. [20](#)
- [38] M. Fei and Y. Liu. Phase-field approximation of the Willmore flow. *Arch. Ration. Mech. Anal.*, 241(3):1655–1706, 2021. [5](#)
- [39] H. Gomez and T. J. R. Hughes. Provably unconditionally stable, second-order time-accurate, mixed variational methods for phase-field models. *J. Comput. Phys.*, 230(13):5310–5327, 2011. [20](#)
- [40] D. Hou, M. Azaiez, and C. Xu. A variant of scalar auxiliary variable approaches for gradient flows. *Journal of Computational Physics*, 395:307–332, 2019. [21](#)
- [41] F. Huang, J. Shen, and Z. Yang. A highly efficient and accurate new scalar auxiliary variable approach for gradient flows. *SIAM Journal on Scientific Computing*, 42(4):A2514–A2536, 2020. [21](#)
- [42] Q.-A. Huang, W. Jiang, J. Z. Yang, and C. Yuan. A structure-preserving, upwind-SAV scheme for the degenerate Cahn–Hilliard equation with applications to simulating surface diffusion, 2023. [21](#)
- [43] L. Ju, X. Li, and Z. Qiao. Generalized SAV-exponential integrator schemes for Allen–Cahn type gradient flows. *SIAM Journal on Numerical Analysis*, 60(4):1905–1931, 2022. [21](#)
- [44] Z. Liu and X. Li. The exponential scalar auxiliary variable (E-SAV) approach for phase field models and its explicit computing. *SIAM Journal on Scientific Computing*, 42(3):B630–B655, 2020. [21](#)
- [45] P. Loreti and R. March. Propagation of fronts in a nonlinear fourth order equation. *European J. Appl. Math.*, 11(2):203–213, 2000. [5](#)
- [46] L. Modica and S. Mortola. Il limite nella Γ -convergenza di una famiglia di funzionali ellittici. *Boll. Un. Mat. Ital. A (5)*, 14(3):526–529, 1977. [2](#)
- [47] L. Modica and S. Mortola. Un esempio di Γ -convergenza. *Boll. Un. Mat. Ital. B (5)*, 14(1):285–299, 1977. [2](#)
- [48] R. Moser. A higher order asymptotic problem related to phase transitions. *SIAM J. Math. Analysis*, 37(3):712–736, 2005. [4](#), [10](#)
- [49] D. Mumford and J. Shah. Optimal approximations by piecewise smooth functions and associated variational problems. *Comm. Pure Appl. Math.*, 42(5):577–685, 1989. [5](#)
- [50] Y. Nagase and Y. Tonegawa. A singular perturbation problem with integral curvature bound. *Hiroshima Mathematical Journal*, 37:455–489, 2007. [4](#), [10](#)
- [51] M. Röger and R. Schätzle. On a modified conjecture of De Giorgi. *Math. Z.*, 254(4):675–714, 2006. [2](#), [4](#), [10](#)
- [52] C.-B. Schönlieb and A. Bertozzi. Unconditionally stable schemes for higher order inpainting. *Communications in Mathematical Sciences*, 9:413–457, 06 2011. [20](#)

- [53] J. Shen, J. Xu, and J. Yang. The scalar auxiliary variable (SAV) approach for gradient flows. *Journal of Computational Physics*, 353:407–416, 2018. [21](#)
- [54] J. Shen, J. Xu, and J. Yang. A new class of efficient and robust energy stable schemes for gradient flows. *SIAM Review*, 61(3):474–506, 2019. [21](#)
- [55] J. Shin, H. G. Lee, and J.-Y. Lee. First and second order numerical methods based on a new convex splitting for phase-field crystal equation. *J. Comput. Phys.*, 327:519–542, 2016. [20](#)
- [56] J. Shin, H. G. Lee, and J.-Y. Lee. Unconditionally stable methods for gradient flow using convex splitting Runge-Kutta scheme. *J. Comput. Phys.*, 347:367–381, 2017. [20](#)
- [57] Y. Tonegawa. Phase field model with a variable chemical potential. *Proceedings of the Royal Society of Edinburgh: Section A Mathematics*, 132:993–1019, 7 2002. [4](#)
- [58] R. Wang, Y. Ji, J. Shen, and L.-Q. Chen. Application of scalar auxiliary variable scheme to phase-field equations. *Computational Materials Science*, 212:111556, 2022. [21](#)
- [59] X. Wang. Asymptotic analysis of phase field formulations of bending elasticity models. *SIAM J. Math. Anal.*, 39(5):1367–1401, 2008. [5](#)
- [60] S. M. Wise, C. Wang, and J. S. Lowengrub. An energy-stable and convergent finite-difference scheme for the phase field crystal equation. *SIAM J. Numer. Anal.*, 47(3):2269–2288, 2009. [20](#)
- [61] Z. Yang, L. Lin, and S. Dong. A family of second-order energy-stable schemes for Cahn–Hilliard type equations. *Journal of Computational Physics*, 383:24–54, 2019. [21](#)
- [62] Y. Zhang and J. Shen. A generalized SAV approach with relaxation for dissipative systems. *Journal of Computational Physics*, 464:111311, 2022. [21](#)

INSA LYON, CNRS, ECOLE CENTRALE DE LYON, UNIVERSITÉ CLAUDE BERNARD LYON 1, UNIVERSITÉ JEAN MONNET, ICJ UMR5208, 69621 VILLEURBANNE, FRANCE, ELIE.BRETIN@INSA-LYON.FR

CEREMADE, CNRS, UNIVERSITÉ PARIS-DAUPHINE, PSL UNIVERSITY, PARIS, MOKAPLAN, INRIA, PARIS, FRANCE, CHAMBOLLE@CEREMADE.DAUPHINE.FR.

UNIVERSITÉ CLAUDE BERNARD LYON 1, CNRS, ECOLE CENTRALE DE LYON, INSA LYON, UNIVERSITÉ JEAN MONNET, ICJ UMR5208, 69622 VILLEURBANNE, FRANCE, MASNOU@MATH.UNIV-LYON1.FR